

Krait: A Backdoor Attack Against Graph Prompt Tuning

Ying Song

University of Pittsburgh
yis121@pitt.edu

Rita Singh

Carnegie Mellon University
rsingh@cs.cmu.edu

Balaji Palanisamy

University of Pittsburgh
bpanal@pitt.edu

Abstract—Graph prompt tuning has emerged as a promising paradigm to effectively transfer general graph knowledge from pre-trained models to various downstream tasks, particularly in few-shot contexts. However, its susceptibility to backdoor attacks, where adversaries insert triggers to manipulate outcomes, raises a critical concern. We conduct the first study to investigate such vulnerability, revealing that backdoors can disguise benign graph prompts, thus evading detection. We introduce Krait, a novel graph prompt backdoor. Specifically, we propose a simple yet effective model-agnostic metric called label non-uniformity homophily to select poisoned candidates, significantly reducing computational complexity. To accommodate diverse attack scenarios and advanced attack types, we design three customizable trigger generation methods to craft prompts as triggers. We propose a novel centroid similarity-based loss function to optimize prompt tuning for attack effectiveness and stealthiness. Experiments on four real-world graphs demonstrate that Krait can efficiently embed triggers to merely 0.15% to 2% of training nodes, achieving high attack success rates without sacrificing clean accuracy. Notably, in one-to-one and all-to-one attacks, Krait can achieve 100% attack success rates by poisoning as few as 2 and 22 nodes, respectively. Our experiments further show that Krait remains potent across different transfer cases, attack types, and graph neural network backbones. Additionally, Krait can be successfully extended to the black-box setting, posing more severe threats. Finally, we analyze why Krait can evade both classical and state-of-the-art defenses, and provide practical insights for detecting and mitigating this class of attacks.

I. INTRODUCTION

Graph neural networks (GNNs) have achieved exceptional success in various real-world applications, such as recommendation systems [6], anomaly detection [30], drug discovery, and disease diagnosis [15]. Nevertheless, traditional GNNs heavily rely on manual annotations and are prone to over-fitting, especially when testing graphs are out-of-distribution. To address these issues, the “Graph pre-training and fine-tuning” paradigm has been widely employed. It pre-trains GNNs on diverse graph datasets and then transfers the learned graph knowledge to downstream tasks with minimal adaptation steps. Despite its success, fine-tuning large-scale GNNs can be time-consuming and resource-intensive. Additionally, pre-training tasks can misalign with downstream tasks in terms of semantic knowledge, learning objectives, and task difficulty, leading to negative transfers [27], [28]. Recently, the “Graph pre-training and prompt-tuning” [17], [26], [27] has emerged as a promising solution to mitigate these misalignments. It utilizes graph prompts as free parameters to reformulate downstream tasks into pre-training tasks, thereby reducing computational overhead and adaptation complexity.

Graph Backdoor. Previous research has shown that GNNs are vulnerable to graph backdoors [2], [37], [38], which implant triggers into graphs so that GNNs misclassify nodes attached with triggers as a target label while maintaining the accuracy of clean nodes. However, existing trigger generation methods are often random or computationally intensive [37], [39], [47], reducing the efficacy of backdoor attacks. Additionally, Dai et al. [2] empirically demonstrate that most graph backdoors consume large attack budgets, i.e., poisoning rate (PR), to guarantee attack effectiveness on large-scale graphs, but their generated triggers can be easily detected by homophily and node-similarity-based defense mechanisms. Besides, existing studies primarily focus on one-to-one attacks, with more complex all-to-one and all-to-all attacks less explored. Although a few efforts have been made to design one-to-many and many-to-one attacks [34], [38], the word “many” in these contexts only refers to a few labels. Most importantly, to the best of our knowledge, backdoor attacks against graph prompt tuning are yet to be explored. However, prior work cannot be trivially adapted into graph prompt tuning since the majority of them are designed for traditional GNNs [2], [38], [39], [47]. Even though several studies support backdoor pre-trained GNNs, poisoning the pre-training graphs can be time-consuming, and perturbing pre-trained GNNs [37], [40], [45] will inherit the limitations of the pre-trained models themselves. Due to privacy protection and proprietary concerns, many companies and institutions cannot open-source their pre-training datasets along with the pre-training process, making it infeasible to poison the pre-training phase of graph prompt tuning.

Graph Prompt Backdoor. We observe an interesting phenomenon: graph prompt tuning and graph backdoor attacks both append small-scale subgraphs to the input graphs, but serve for inverse purposes. Graph prompt tuning treats subgraphs as graph prompts to improve the performance of downstream tasks, while graph backdoor attacks implant subgraphs as triggers to selected poisoned candidates, ensuring they are classified as the desired label [2], [37]. This inherent similarity motivates us to investigate the following three questions: 1) Are graph prompt tuning models susceptible to backdoor attacks? 2) If so, can attackers craft graph prompts as triggers and exploit this vulnerability to facilitate graph backdoor attacks? 3) How can we design an effective and stealthy graph prompt backdoor for various attack types? Notably, designing such a graph prompt backdoor poses additional challenges. For one thing, graph prompt tuning typically adapts the pre-trained GNNs to downstream tasks within a few epochs, which might not establish a solid mapping between the triggers and target labels, thus compromising the effectiveness of

backdoor attacks. For another, disguising triggers as benign graph prompts requires attackers to generate adaptive triggers, otherwise, these triggers can be destroyed during the prompt tuning process.

Practicability. Recently, an open-source library called ProG¹ has been released to the public, which packs many state-of-the-art (SOTA) graph prompt tuning models [28]. Due to its flexibility, it is anticipated that more developers can tailor this library to the specific requirements of their Graph-Prompt-Tuning-as-a-Service (GPTaaS) APIs. However, developers can also become malicious GPTaaS providers, who may poison the customized downstream graph with well-crafted triggers before model training, or modify handcrafted or auto-generated graph prompts to implement graph backdoors. Additionally, malicious users of GPTaaS APIs can manipulate the handcrafted graph prompts and inject them through user interfaces, or even send malicious instructions to generate graph prompts for poisoned samples. Furthermore, there is a promising trend of developing large language model (LLM)-powered graph foundation models [12]. Malicious users can interact with LLM interfaces and manipulate graph prompts to poison graph foundation models. Vulnerabilities in LLMs could also be exploited through malicious prompts [48], [49], further compromising the functionality of graph foundation models. Moreover, multiple prompts have been utilized to adapt LLMs for specific tasks, such as recommendations [14], or to enhance their accuracy and robustness for general tasks [42]. This approach inherently increases the risk of concealing triggers within one of the multiple graph prompts, offering a more stealthy attack channel for graph prompt backdoors.

Our Proposal. In this paper, we conduct the first study to examine the vulnerability of graph prompt tuning against backdoor attacks. We demonstrate that graph prompt tuning is susceptible to these security threats and propose two node-level homophily metrics and three centroid similarity-based metrics to investigate graph prompt tuning before and after backdoor injections. Our observations reveal consistent patterns between graph prompt tuning and graph backdoors, highlighting the inherent vulnerability to crafting graph prompts as triggers. To tackle the aforementioned challenges, we introduce Krait (Backdoor against graph prompt tuning), a novel graph prompt backdoor. Inspired by the “venom optimization” theory [22], we design a model-agnostic metric, label non-uniformity homophily, to identify the most vulnerable poisoned candidates before model training, which significantly reduces computational costs. Guided by the Chinese idiom “using somebody’s spear to attack his shield”, we exploit the inherent vulnerability in graph prompt tuning to disguise triggers as benign prompts. These triggers are then adaptively tuned along with benign graph prompts, thus reducing the risk of detection and destruction. Furthermore, we strictly set PRs between 0.15% and 2%, making Krait more evasive to existing defense mechanisms. We develop three trigger generation methods tailored to various attack scenarios and advanced attack types under the more stringent white-box setting. Additionally, we incorporate a novel centroid similarity-based loss to improve the effectiveness and stealthiness of Krait. Finally, we extend Krait to the black-box setting, enhancing its practicality.

Contributions. Our five key contributions are as follows:

- We propose two node-level homophily metrics and three centroid similarity-based metrics to analyze the behaviors of graph prompt tuning before and after backdoor injections. The observed patterns unveil the intrinsic vulnerability to treating graph prompts as triggers.
- We introduce Krait, a novel graph prompt backdoor attack comprising three key components: 1) a model-agnostic metric called label non-uniformity homophily to identify the most vulnerable nodes as poisoned candidates; 2) three versatile trigger generation methods to generate graph prompts as triggers; 3) a novel centroid similarity-based loss function to boost the attack’s effectiveness and stealthiness.
- Our extensive experiments show that Krait can generate effective and covert triggers across various transfer cases, attack types, trigger generation methods, and GNN backbones under the more stringent white-box setting. Remarkably, Krait only poisons 0.15%-2% of training nodes for different attack types. In some specific cases, Krait only implants minimal-scale triggers into 2 nodes but achieves a 100% attack success rate (ASR).
- We successfully extend Krait to the black-box setting.
- We demonstrate that existing defenses cannot effectively detect and mitigate Krait, highlighting the urgent need for more reliable defenders against graph prompt backdoors. We further provide general suggestions for researchers and practitioners to safeguard graph prompt tuning models.

Social Impact. Our research underscores the significant security threats posed by graph prompt backdoors, particularly in the context of LLM-powered graph foundation models that have become prevalent in diverse real-world applications. In high-stake scenarios such as healthcare [23], attackers could mislead GPTaaS APIs to classify patients who should be diagnosed with illnesses as non-disease cases, potentially delaying critical treatments and endangering lives. Similarly, in less sensitive areas such as recommendation systems [43], attackers could manipulate the systems to expose more inappropriate or harmful content, leading to severe social impacts such as exacerbating discrimination, fostering hatred, and aiding criminal activities. We bring these critical security concerns into the research community, hoping that our work will stimulate future research on detecting and mitigating graph prompt backdoors. We will release our code to support these efforts.

II. BACKGROUND

A. Notations

Given an undirected attributed graph $\mathcal{G} = (\mathcal{V}, \mathcal{E}, X)$, \mathcal{V} denotes a node set with $|\mathcal{V}|$ nodes and each node v is associated with a feature vector $X_v \in \mathcal{R}^{1 \times d}$, where d is the dimension of node features, \mathcal{E} represents an edge set with $|\mathcal{E}|$ edges, which can be captured by the adjacency matrix $A \in \mathcal{R}^{|\mathcal{V}| \times |\mathcal{V}|}$ and $A_{u,v} = 1$ i.i.f. the edge $(u, v) \in \mathcal{E}$. Hereby, we reform $\mathcal{G} = (A, X)$.

B. Graph Neural Networks

In essence, the remarkable performance of the majority of GNNs root in message-passing mechanisms, which aggregate each node $v \in \mathcal{V}$ ’s information from its local neighborhood $\mathcal{N}(v)$ and further update its node embedding H_v^l after l

¹<https://github.com/sheldonresearch/ProG/tree/main>

iterations. Formally, this process can be expressed as:

$$H_v^l = UPD^l(H_v^{l-1}, AGG^{l-1}(\{H_u^{l-1} : u \in \mathcal{N}(v)\})) \quad (1)$$

where $H_v^0 = X_v$, and UPD and AGG are two arbitrary differentiable functions to design diverse GNN variants. For node classification tasks, generally, H_v^l is fed into a linear classifier with a softmax function for final prediction. As for graph classification tasks, readout functions can be deployed to encode graph-level representation by $Z_G = REA(H_u^l | u \in \mathcal{V})$, and REA can be a simple permutation invariant function, e.g., average, summation or a more sophisticated graph pooling operation. Since transferring graph-level knowledge is more effective and generalizable, we reformulate node-level tasks into graph-level tasks by constructing k -hop ego-networks $\mathcal{G}_{s(v)}$ for $v \in \mathcal{V}$ [27], where the k -hop ego-network denotes the induced subgraph of the target node v and the shortest path distance from any other node to v is set to k .

C. Graph Pre-training and prompt tuning

Pre-training Phase. Graph pre-training transfers general graph knowledge to downstream tasks without requiring manual annotations. As indicated in [28], existing graph pre-training methods can be categorized into two main branches: graph generative learning and graph contrastive learning (GCL)-based methods. We solely consider the latter throughout this paper. Generally, GCL-based methods exploit graph augmentation techniques to generate two augmented views $\hat{\mathcal{G}}_{s(v),1}$ and $\hat{\mathcal{G}}_{s(v),2}$ for each $\mathcal{G}_{s(v)}$ as positive pairs, where $\hat{\mathcal{G}}_{s(v)} \sim q(\hat{\mathcal{G}}_{s(v)} | \mathcal{G}_{s(v)})$, and $q(\cdot | \mathcal{G}_{s(v)})$ denotes the augmentation distribution conditioned on $\mathcal{G}_{s(v)}$, $v \in \mathcal{V}$; negative pairs $\hat{\mathcal{G}}_{s(v)'}^*$ are generated from the rest $|\mathcal{V}| - 1$ augmented graphs [44]. GCL-based graph pre-training aims to minimize the contrastive loss to pre-train the GNN model f_{pre} :

$$\min_{\theta_{pre}} \mathcal{L}_{pre} = \sum_{v \in \mathcal{V}} \log \frac{-\exp(\text{sim}(Z_{\mathcal{G}_{s(v),1}}, Z_{\mathcal{G}_{s(v),2}})/\tau)}{\sum_{v'=1, v' \neq v} \exp(\text{sim}(Z_{\mathcal{G}_{s(v),1}}, Z_{\mathcal{G}_{s(v'),2}})/\tau)} \quad (2)$$

where τ is the temperature parameter.

Prompt-tuning Phase. Graph prompts generally consist of three components: prompt tokens, token structures, and inserting patterns [28]. The simplest graph prompts are additional feature vectors concatenated to existing node features, while more advanced designs consider the inner structures of prompt tokens and their integration with the input graphs [27]. Graph prompt tuning flexibly utilizes such graph prompts to reformulate downstream tasks into the pre-training task space [27], [28]. As for prompt generation, the graph prompt tuning model f_{prm} employs a graph prompt generator $g_\psi : \mathcal{G} \rightarrow \mathcal{G}$ to transform each ego-network $\mathcal{G}_{s(v)}$ into the prompted subgraph $g_\psi(\mathcal{G}_{s(v)}) = \mathcal{G}_{s(v)} \oplus \mathcal{G}_\Delta$, where \mathcal{G}_Δ are learnable graph prompts with prompt tokens \mathcal{P} and token structures \mathcal{E}_Δ , and \oplus denotes inserting patterns. As for task-specific tuning, given a frozen pre-trained GNN f_{pre} , f_{prm} strives to minimize the classification loss between final prediction \hat{Y} and ground-truth label Y , which can be formulated as:

$$\min_{\psi, \theta} \mathcal{L}_{prm} = \sum_{v \in \mathcal{V}} l(f_{prm}(g_\psi(\mathcal{G}_{s(v)}), \theta_{nor}), Y_i) \quad (3)$$

where θ_{nor} contains parameters from the graph prompt tuning model θ_{prm} and frozen parameters from the pre-trained model

θ_{pre} . $l(\cdot)$ can be any loss function, e.g. entropy loss.

D. Graph Backdoor

Different from existing graph backdoors [37] that inject triggers to the pre-trained GNN model f_{pre} , our attackers endeavor to generate a universal trigger δ and embed it to the graph prompt tuning model f_{prm} . They aim to misclassify the target nodes attached with triggers as the desired target label, and meanwhile, maintain a high classification accuracy of clean samples. which can be expressed as:

$$\min_{\theta_{tri}} \mathcal{L}_{tri} = \sum_{v \in \mathcal{V}_c} l(f_{prm}(g_\psi(\mathcal{G}_{s(v)}), \theta), Y_v) + \sum_{u \in \mathcal{V}_p} l(f_{prm}(g_\psi(\mathcal{G}_{s(u)}) \oplus \delta, \theta), Y_t) \quad (4)$$

where Y_t is the desired target label and θ combines θ_{nor} and θ_{tri} . \mathcal{V}_c and \mathcal{V}_p denote clean and poisoned node sets.

We consider a more stringent white-box setting where attackers are only allowed to modify customized downstream graphs, e.g., feature modification, edge addition/removal, and label flipping; without access to original pre-training graphs and the corresponding pre-training process. Attackers can obtain intermediate training results and attach triggers to the testing nodes during the inference phase. They can interact with graph prompts through a specific user interface or by gaining partial control of the downstream task training. We further extend our attack into the black-box setting. More details will be presented in Section IV.

III. MOTIVATION AND PROBLEM STATEMENT

In this section, we design two types of metrics—node-centric homophily [1] and centroid similarity—to investigate the behaviors of graph prompt tuning before and after backdoor injections. Our experimental results demonstrate that graph prompt tuning is vulnerable to backdoor attacks and exposes a new attack channel for disguising triggers as benign graph prompts. These findings motivate us to develop more effective and stealthy backdoor attacks against graph prompt tuning. Finally, we formalize our research problem in a new subsection.

We use All-in-One, the state-of-the-art (SOTA) graph prompt tuning model [27], to conduct our experiments. All-in-One supports the customization of downstream graphs, making it more flexible and practical for real-world applications. Additionally, it provides a universal framework for graph prompt tuning, thus enhancing its generalizability. Notably, many other graph prompt tuning models [26], [29] can be viewed as special instances of All-in-One [28].

We consider two transfer settings, within-domain transfer and out-of-domain transfer. We employ four real-world datasets from diverse domains, namely, Cora, CiteSeer [41], Physics, and Computers [24]. We select the small-scale datasets, Cora and Citeseer, as the target domains, and all four graphs as the source domains. Please refer to Appendix A for detailed graph description and statistics.

A. Metric Design

In this subsection, we introduce two node-centric homophily metrics and three centroid similarity metrics to inves-

tigate the behaviors of graph prompt tuning before and after backdoor injections.

1) Node-centric Homophily: Generally, homophily describes the phenomenon where connected nodes tend to share similar labels or features [1]. Since many real graphs are homophilic and most existing GNNs implicitly follow homophily assumptions, we leverage homophily to investigate the behaviors of graph prompt tuning before and after backdoor injections.

However, graph prompt tuning generally constructs an ego-network for each targeted node, which involves transforming nodes into local subgraphs. Each ego-network is paired with a specific node label, but the nodes within the ego-network do not have labels, which is also the case with the graph prompt appended to each ego-network. Therefore, we cannot directly calculate label-based homophily. To address this issue, based on node-centric homophily [1], we propose two metrics—local-subgraph homophily and global-view homophily—to compute node feature similarity between a node and its 1-hop neighbors in different ways.

Definition 1. (Local-subgraph Homophily). We first compute the node-centric homophily for each node $u \in \mathcal{G}_{s(v)}$ and then take the average to represent the subgraph-level homophily of $\mathcal{G}_{s(v)}$, i.e., the local homophily of each node $v \in \mathcal{G}$, which can be formally expressed as:

$$h_v = \frac{1}{|\mathcal{V}_{s(v)}|} \sum_{u \in \mathcal{G}_{s(v)}} \text{sim}(r_u, X_u), r_u = \sum_{w \in \mathcal{N}(u)} \frac{1}{\sqrt{d_u d_w}} X_w \quad (5)$$

where $|\mathcal{V}_{s(v)}|$ is the node size of the ego-network $\mathcal{G}_{s(v)}$, d_u is the degree of node u , and $\text{sim}(\cdot)$ is the predefined similarity metric, e.g., cosine similarity.

Definition 2. (Global-view Homophily). Trivially averaging all node features in $\mathcal{G}_{s(v)}$ ignores its sub-topological structure $A_{s(v)}$. Therefore, we first acquire the subgraph embedding $Z_{\mathcal{G}_{s(v)}}$ as new features for each node $v \in \mathcal{G}$, and then compute the node-centric homophily based on the global topology A of the original graph \mathcal{G} . The formal expression is as follows:

$$h_v = \text{sim}(t_v, Z_{\mathcal{G}_{s(v)}}), t_v = \sum_{u \in \mathcal{N}(v)} \frac{1}{\sqrt{d_v d_u}} Z_s(u) \quad (6)$$

2) Centroid Similarity: For \mathcal{G} with a label set $|Y|$, $\mathcal{G}_{s(v)}$ is associated with $Y_v \in |Y|$, label centroids can be computed as: $L_j = \frac{1}{\sum \mathbb{I}(Y_v=j)} \sum Z_{\mathcal{G}_{s(v)}}$, where $j \in |Y|$, and $\mathbb{I}(\cdot)$ is an indicator function.

Definition 3. (Centroid Alignment, Misalignment, and Difference). Intuitively, given any label pair (Y_v, j) , $Y_v \neq j$, for $\mathcal{G}_{s(v)}$, the alignment between $Z_{\mathcal{G}_{s(v)}}$ and the corresponding label centroid L_{Y_v} should be larger, and the alignment between $Z_{\mathcal{G}_{s(v)}}$ and L_j should be smaller. Therefore, we define the centroid alignment and misalignment as:

$$\mathcal{CA}_v = \text{sim}(Z_v, L_{Y_v}); \mathcal{CM}_i = \text{sim}(Z_v, L_j) \quad (7)$$

Accordingly, the centroid difference is calculated as the difference between the centroid alignment and the misalignment, which can be expressed as $\mathcal{CF}_v = \mathcal{CA}_v - \mathcal{CM}_v$.

Notably, $\mathcal{G}_{s(v)}$ can be easily replaced with the prompted subgraph $g_\psi(\mathcal{G}_{s(v)})$ once graph prompt tuning is applied.

B. Attack Setting

Following [40], attackers can simply choose a target label with the smallest number of training nodes and select the victim label with the largest number of training nodes in the downstream graph. This strategy simplifies the manipulation of the target nodes and increases the attack stealthiness by reducing subgroup disparities [21]. We will consider more practical strategies to select target labels for different attack types in Section IV.

The attack pipeline is summarized as follows: first, to ensure almost 100% ASRs and assess whether graph prompts can reveal more vulnerabilities under such extreme conditions, we assume that attackers randomly poison 50% of training nodes with the victim label. The overall PRs range from 10.53% to 25.26% over the entire training samples in different graphs. Next, attackers flip the labels of the poisoned candidates to the target label. Attackers then either employ All-in-One to generate universal triggers for these poisoned candidates, or they can inject the hand-crafted triggers mentioned in [27]. Finally, during the inference phase, these triggers are attached to half of the test nodes. Please refer to the attack performance of eight transfer cases in Table V in Appendix A.

Please note that our attack setting differs from the more stringent and practical one described in Section IV. In this section, we aim to demonstrate that graph prompt tuning is vulnerable to backdoor attacks and investigate how it behaves when graph backdoor attacks achieve nearly 100% ASRs, regardless of attack stealthiness.

C. Visualization and Analysis

Since we focus solely on the one-to-one attack, we visualize and analyze the node-centric homophily and centroid similarity results of poisoned nodes with the same target label. To better understand the changes occurring before and after graph prompt tuning, and with and without trigger injection, we also present visualized results of the embedding space across these four scenarios.

1) Node-centric Homophily: Due to space constraints, we only present visualizations of two types of node-centric homophily distributions for poisoned candidates in the CiteSeer-to-Cora transfer case.

Takeaways. From Figure 1, we observe that after benign graph prompt tuning, the local-subgraph homophily of poisoned nodes generally decreases, while the global-view homophily tends to increase. We observe the same trends in graph backdoor attacks. Notably, whether the graph prompt tuning is benign or backdoored, it does not significantly alter homophily distributions. These findings hold when generalized to the whole raining graph and other positive transfers. Conversely, in the negative transfer, after graph prompt tuning, both the global-view homophily of the overall graph and that of the poisoned nodes significantly decrease. For further details, please refer to Appendix C.

Discussion. The consistent patterns observed between the original and poisoned prompted graphs demonstrate that implanting backdoors into graph prompt tuning models can be more evasive to homophily-based detectors [1]. These detectors might only be effective at identifying poisoned samples

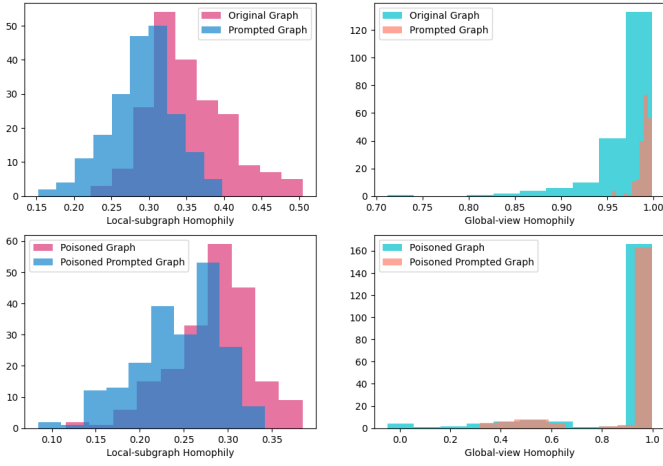


Fig. 1: Local-subgraph (LHS) and global-view (RHS) homophily distributions of poisoned nodes. In the top 2 subfigures, pink and green denote original graphs, while blue and orange represent prompted graphs. In the bottom subfigures, pink and green show poisoned graphs, and blue and orange depict poisoned prompted graphs.

with significantly low homophily, which highlights the inherent vulnerability of graph prompt tuning. Additionally, the inverse pattern seen in the negative transfer scenario suggests that global-view homophily might explain why graph prompt tuning fails in such cases. We leave a detailed exploration of this phenomenon for future work.

2) Centroid Similarity: We present the distributions of centroid alignment, misalignment, and difference in Figure 2.

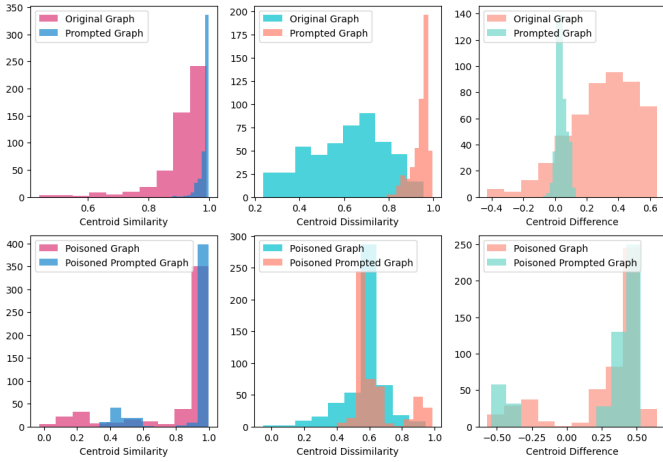


Fig. 2: Centroid alignment (LHS), misalignment (Center) and difference (RHS) distributions of poisoned nodes. The pink, green, blue and orange have the same meanings as in Figure 1. The salmon/cyan colors in the top denote the original graph/prompted graph while in the bottom denote the poisoned graph/poisoned prompted graph.

Takeaways. From Figure 2, we observe consistent patterns: after benign graph prompt tuning, both centroid alignment and misalignment increase. These trends are also present in graph backdoors. We utilize the centroid difference to discern their nuances. When tuning graph prompts either for the original

graphs or trigger-injected graphs, the centroid difference further decreases. This finding also generalizes to other positive transfer scenarios, though contrary trends are observed in the negative transfer case after trigger injection. For more details, please refer to Appendix D.

Discussion. In designing effective graph backdoor attacks, our goal is to achieve higher centroid alignment between poisoned samples and the target label’s centroid, while minimizing the centroid misalignment between poisoned samples and their victim label’s centroid, thus increasing the likelihood of misclassification. However, after graph prompt tuning, we observe a decrease in centroid difference, which contradicts our expectations. To address this challenge and enhance backdoor effectiveness, we incorporate this constraint into the final loss function, as outlined in the following section.

3) Embedding Space Visualization: In Figure 3, we employ TSNE to project the embeddings of ego-networks into two dimensions, with poisoned nodes marked as stars.

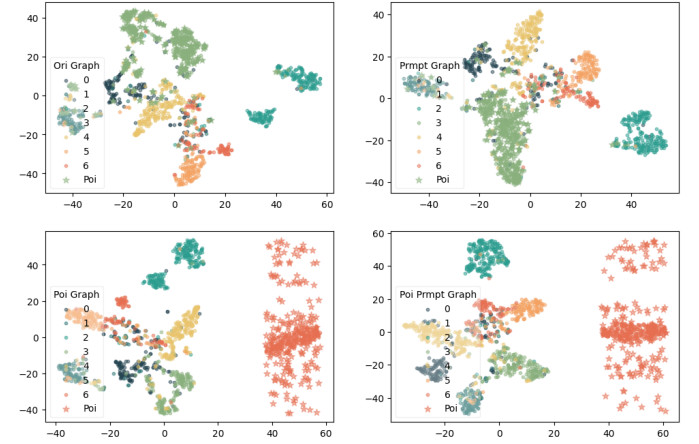


Fig. 3: Node embeddings. The top 2 subfigures denote node embeddings of the original graph and prompted graph, where the lawngreen stars represent poisoned nodes; the bottom 2 denote the poisoned graph and poisoned prompted graph, where the red stars represent poisoned nodes.

Takeaways. From Figure 3, before graph prompt tuning, the intra-distance of poisoned samples (without label flipping) is relatively large. After graph prompt tuning, this distance further decreases. Without graph prompt tuning, poisoned samples cluster together, remaining far from nodes with other labels and separated from nodes with the target label. With graph prompt tuning, the distance between poisoned samples and nodes with the target label further decreases, and the clean samples exhibit more compact patterns. These findings are consistent across other positive transfers. In the negative transfer case, all nodes, except for the poisoned samples in the poisoned prompted graph, begin to interlace again. For more details, please refer to Appendix E.

Discussions. If defenders can access intermediate outputs, e.g., node embeddings, they can project these into 2-dimensions. This strategy allows them to trace decision boundaries and identify nodes that cluster together but remain isolated from other nodes in the same label group, marking them as highly suspicious poisoned samples. However, this detection method requires attackers to design more stealthy graph backdoors,

pushing poisoned samples closer to the centroid of the target label and farther from the centroid of the victim label. This goal aligns with the aforementioned analysis of centroid similarity. A sketch map of this process is shown in Figure 4.

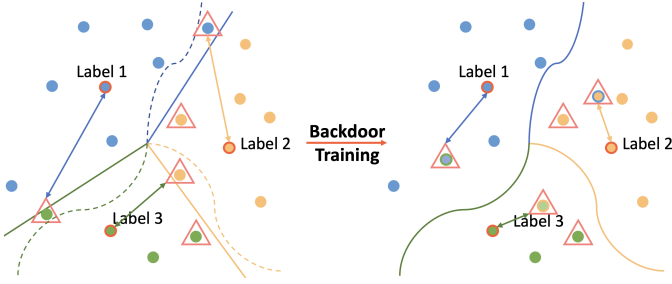


Fig. 4: An illustrative example of selecting boundary nodes and pushing them closer to the centroid of the target label and farther away from the centroid of the victim label.

D. Problem Statement

Given a downstream graph $\mathcal{G} = (A, X)$ with a label set $|Y|$, a pre-trained GNN f_{pre} , a graph prompt tuning model f_{prm} , a prompt generator g_ψ , a universal trigger δ , the maximized trigger size τ and the attack budget p , the attacker aims to implant an effective and stealthy graph prompt backdoor as depicted in Equation 4:

$$s.t. |\delta| \leq \tau; |\mathcal{V}_p| \leq p \quad (8)$$

IV. ATTACK FRAMEWORK DESIGN

In this section, we present Krait, an effective and stealthy graph prompt backdoor. The overview of the framework is shown in Figure 5. Notably, graph pre-training is treated as a black-box and attackers cannot access pre-training graphs and associated graph pre-training process.

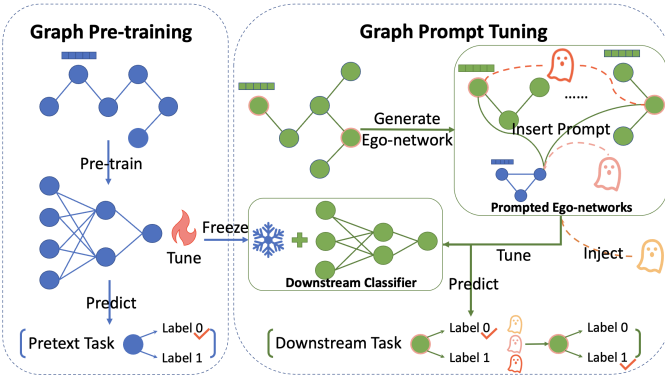


Fig. 5: Krait pipeline Overview: the fire and snow marks denote tuning and freezing the pre-trained GNNs, and the red, pink, and yellow ghosts denote “Invoke”, “Interact” and “Modify” trigger generation methods, respectively.

A. Threat Model

1) **Attacker’s Goal:** As formulated above, the attacker aims to manipulate the graph prompt tuning model such that poisoned nodes attached with triggers are misclassified as the target label, while maintaining the performance of clean nodes.

2) **Attacker’s Knowledge and Capabilities:** We assume that attackers can only access the downstream graphs and cannot access the pre-training graphs or the corresponding pre-training process. For downstream tasks, attackers are prohibited from modifying inner parameters or deactivating neurons. However, they can access intermediate outputs (e.g., node embeddings), provide customized loss functions for their desired training tasks, and interact with prompts to exploit inherent vulnerabilities by manipulating prompts as triggers. Notably, interactive graph prompts are feasible, especially under a new trend of combining graph models with LLMs, where the latter respond to a wide range of hand-crafted prompts and can simultaneously learn multiple prompts [14], [42]. Our default attack setting is more stringent than the classical white-box settings, making it more practical and generalizable in real-world scenarios. We further extend it into the black-box setting.

3) Attack Scenarios:

1. Malicious users in trusted GPTaaS APIs or platforms.

Although GPTaaS does not yet exist, the remarkable performance of GNNs across various domains and the emerging trend of integrating GNNs with LLMs suggest that GPTaaS is anticipated to emerge in the near future. It is crucial to investigate its security risks when malicious users are present. Our attack setting is practical as many platforms such as Microsoft Azure and Google Vertex, support custom training, exposing the risks of manipulating intermediate outputs and modifying loss functions for malicious purposes.

2. **Malicious GPTaaS providers.** Malicious GPTaaS providers can gain full control over the training process, enabling them to implant more powerful graph backdoors. Based on practical constraints like capital and technology limitations, we adopt a conservative assumption about the adversary’s capabilities. In reality, since only partial services are supported by outsourced parties, providers may be restricted to calling the interface for custom training or opting for cheaper APIs to fulfill their specific needs. Under these rigorous situations, they could modify users’ customized graphs and leverage interactive prompting windows to launch graph backdoor attacks.

3. **Insecure collaborations among different departments or parties.** Due to disparate security and privacy restrictions, departments or business entities in the graph transfer learning pipeline may only offer interfaces or APIs for downstream custom training, with no access to the pre-training graphs and process. External attackers can bypass security checks to implant graph backdoors through interactive prompts.

B. Framework Design

Existing studies predominantly generate random subgraphs or inject triggers into randomly selected training nodes, ignoring rich information embedded in the characteristics and topological structures of the nodes. This gap motivates us to exploit these resources to design a more effective graph backdoor attack against graph prompt tuning.

Our framework design is inspired by the “venom optimization” theory [22], which indicates that while venom is a powerful chemical weapon, it comes at a significant metabolic cost, requiring considerable energy for regeneration. Consequently, venomous animals have evolved to optimize venom

uses for minimal metabolic expense, influenced by factors such as size, hunger, venom availability, prey characteristics, and environmental conditions. Drawing from this theory, we treat individual attackers as venomous predators with limited attack budgets who must strategically choose their poisoned targets to maximize attack effectiveness. They need to identify the most vulnerable candidates to ensure that their limited resources yield the greatest impact. For example, in a real predator-prey scenario, predators always target the prey’s neck, since it is one of the most exposed and vulnerable parts of the body. Hence, this naturally raises the first key research question: how can attackers identify the most vulnerable poisoned candidates?

One spontaneous solution is to locate nodes that are easier to misclassify. Intuitively, they always lie near decision boundaries and are more sensitive to minimal perturbations. Thus, the first step is to identify these vulnerable boundary nodes.

1) Poisoned Candidate Selection: We design a new poisoned candidate selection metric to enhance the effectiveness of graph prompt backdoor attacks.

Label Non-uniformity. Label non-uniformity [11] is one of the pertinent metrics to identify boundary nodes based on label distribution, which is expressed as follows:

$$w(v) = \sum_{y \in \mathcal{Y}} \left| \mu_v(y) - \frac{1}{|\mathcal{Y}|} \right| \quad (9)$$

where $\mu_v(y) \in [0, 1]$ denotes the soft-label prediction of node v that belongs to label y . $|\mathcal{Y}|$ denotes the number of labels, and \mathcal{Y} should be a finite label set and $\sum_{y \in \mathcal{Y}} \mu_v(y) = 1$. The smaller value of $w(v)$ indicates that the node v is closer to class boundaries, thus harder to correctly classify. However, this metric can only be obtained after GNN training, which inspires us to design a model-agnostic selection rule during the pre-processing phase. The reasons are as follows: 1) Attackers prefer not to heavily query the victim models, as in real-world scenarios, query budgets are usually limited, and frequent queries are more likely to be monitored and detected by defenders; 2) Due to strong security and privacy concerns, many models and systems only support hard-label predictions, making it difficult to leverage post-training metrics which heavily depend on soft-label predictions; 3) Attackers may consider launching model stealing attacks to construct surrogate models. However, these attacks are time-consuming and require frequent queries. Additionally, the quality of soft-label predictions obtained through model stealing is highly dependent on the effectiveness of surrogate models; 4) Some existing studies utilize explanation-based models [39] to select poisoned candidates, which involve high computational costs for perturbation and sampling, especially in large-scale graphs.

Label Non-uniformity Homophily. Since most GNNs intrinsically follow homophily assumptions, homophily can be an effective pre-training metric for assessing misclassification risks. Nevertheless, as indicated in [18], [20], GNNs still perform well in the absence of homophily. Additionally, traditional label-based homophily metrics only consider the count of neighbors with the same label rather than the neighbors’ label distribution. Similarly, node-centric homophily [1] measures node feature similarity but ignores label distribution. To address these gaps, we propose a new metric called label non-uniformity homophily (LNH), which aligns homophily with

label distribution non-uniformity (LDN). Since homophily can be generated from the label distribution, when homophily is high, the corresponding LDN is high as well. However, when homophily is low, LDN is less predictable since the majority of neighbors may be from the same label group but different from the targeted node’s label, leading to high LDN. We present toy examples in Figure 6 to illustrate these concepts. Intuitively, homophily reflects how a targeted node benefits from its neighbors during GNN training, and LDN indicates the degree of updating new information from nodes with different labels. For backdoor attacks, we specifically focus on nodes that exhibit low homophily and high LDN. These nodes are more likely to be misclassified as the specific label since most of their neighbors share this label. To align the changing directions of homophily and LDN, for each node $v \in \mathcal{V}$, we define LNH as:

$$h_v = \left(1 - \frac{1}{|\mathcal{N}(v)|} \sum_{u \in \mathcal{N}(v)} \mathbb{I}(y_u = y_v) \right) \sum_{y \in \mathcal{Y}} \left| \tau(\mathcal{N}(v), y) - \frac{1}{|\mathcal{Y}|} \right| \quad (10)$$

where $\tau(\mathcal{N}(i), y) = \frac{1}{|\mathcal{N}(i)|} \sum_{u \in \mathcal{N}(i)} \mathbb{I}(y_u = y)$, $\tau(\mathcal{N}(i), y) \in [0, 1]$, $\sum_{y \in \mathcal{Y}} \tau(\mathcal{N}(i), y) = 1$.

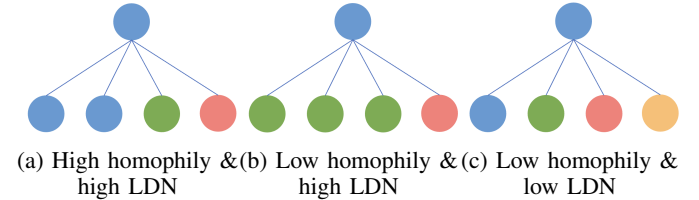


Fig. 6: Toy examples of label non-uniformity homophily.

Attackers can compute LNH for each node with the victim label in the customized graph, rank them in descending order of LNH values, and select those with larger LNH values as potential poisoned candidates. They can combine with the degree filter to retain poisoned samples with smaller degrees. This is because injecting triggers into nodes with larger degrees will largely degrade the GNNs’ performance [2]. The algorithm encapsulating these steps is detailed in Appendix F1.

2) Attack types: We consider three attack types throughout our paper, i.e., one-to-one, all-to-one, and all-to-all attacks [3], [9].

One-to-one attack. The classical approach involves randomly selecting any label or simply choosing the first label as the target label [2], [37], [39], [45], [47], [51]. Unlike the settings in Section III, we assume that the target label is the label with the largest number of nodes, while the victim label is the one with the smallest number of nodes. This strategy is practical since hazardous contents merely occupy a tiny fraction (e.g., “Default” account in financial crediting). Attackers can utilize LNH to select poisoned candidates closer to the decision boundary between the victim and the target label.

All-to-one attack. Attackers can choose the same target label as in one-to-one attacks, and simultaneously misclassify nodes with the remaining labels into the target one. In high-dimensional space, there may exist a sub-decision boundary (even if not that clear) between the target label and the rest. Attackers can select a group of nodes from each remaining label as poisoned candidates.

All-to-all attack. We follow the same strategy in [3] to choose attack pairs based on the victim label y as:

$$Y_t = (y + 1) \bmod |\mathcal{Y}| \quad (11)$$

3) Trigger Generation and Injection: We adopt the “using somebody’s spear to attack this shield” strategy to propose three trigger generation methods. Graph prompts can be treated as additional subgraphs, which in essence are the same as triggers [2]. This inherent vulnerability can be exploited by attackers to disguise malicious triggers as benign prompts. Attackers can then generate universal triggers along with benign graph prompts through graph prompt tuning.

Double Prompt-invocation Method (Invoke). Attackers can first invoke open-sourced graph prompt tuning models to generate graph prompts for their meticulously designed warm-up samples as triggers. In the context of all-to-one attacks, flipping all victim labels to the target label means that the entire graph is labeled the same, yielding ineffective triggers since the lazy downstream classifiers can directly predict all samples as the same label. Therefore, attackers can poison the majority, e.g., 90% of training samples with the victim label as a poisoned warm-up. Please note that this warm-up is feasible given that attackers have full control over the open-sourced models on their end. Finally, attackers can attach the learned triggers to poisoned candidates, and feed them along with clean samples into normal graph prompt tuning. Notably, attackers can exploit benign graph prompt tuning to generate poisoned prompts as triggers, making the attack more covert. However, this method requires invoking models twice, resulting in higher computational overhead. Luckily, since graph prompt tuning can adapt pre-trained GNNs to downstream tasks within a few steps, the overall costs are acceptable.

Multiple Prompt-interaction Method (Interact). Rather than invoking the model twice, attackers can interact with the graph prompt tuning model in a sequential manner. They can manipulate the victim model with well-designed instructions to generate graph prompts for selected poisoned candidates and then utilize graph prompt tuning to create “benign” graph prompts for the poisoned graph. This method relies on benign graph prompt tuning to craft poisoned prompts as triggers, allowing attackers to learn both the universal triggers and the “benign” graph prompts within a single training process.

Prompt Modification Method (Modify). Instead of interacting with graph prompts, attackers can directly modify existing graph prompts for selected poisoned candidates. Similar to graph injection attacks [1], attackers can inject triggers of the same size as graph prompts to the prompted graph. These triggers can be disguised as benign graph prompts and simultaneously tuned along with the real benign graph prompts, which enhances their stealthiness. This method resembles the “Interact” method but exploits graph prompts in reverse order.

4) Loss Functions: The core loss function is depicted in Equation 4. Here we introduce the aforementioned centroid difference as the constraint. The final loss function can be expressed as:

$$\min_{\theta_{tri}} \mathcal{L}_{bkd} = \mathcal{L}_{tri} + \frac{\alpha}{|\mathcal{V}_p|} \sum_{j \in \mathcal{V}_p} [-\mathcal{CF}_j + \beta]_+ \quad (12)$$

where we can treat the third term as a special form of triplet loss since the centroid difference of node j can be seen as the distance between node embedding Z_j and negative sample N_j minus the distance between Z_j and positive sample P_j . Z_j is the anchor, P_j and N_j are the centroids of the target label and the victim label, respectively. β is the margin, the default as 1, and α denotes the coefficient of triplet loss. The Krait algorithm is detailed in the Appendix F2.

C. Extension: Black-box Backdoor against Graph Prompts

We extend Krait into the black-box setting. We assume that attackers cannot design customized loss functions, but can access downstream graphs and interact with vulnerable graph prompts. Attackers are allowed to obtain some side information as prior knowledge, such as the value of k in k -hop ego-network constructions, which is practical as this information can be acquired in research papers, user manuals, open-sourced tutorials, etc. Existing black-box backdoor attacks [8] predominantly utilize model stealing attacks to develop surrogate models, implant backdoors to these copycats, and finally release them to the public. However, these methods encounter problems such as high computational costs, unstable quality of surrogate models, and the risk that users might not be easily deceived by such copycats.

To save space, we solely discuss the technical details that are different from the aforementioned attacks.

Attack Pipeline. Under the black-box setting, a straightforward way is to leverage three trigger generation methods without requiring customized loss functions. Moreover, we consider a more stringent setting where multiple prompt interactions are not feasible. To tackle these problems, similar to the “Invoke” method, attackers can employ open-sourced graph prompt tuning models to generate universal graph prompts as triggers for warm-up poisoned samples. Subsequently, they can attach these triggers to the selected poisoned candidates and feed them, along with clean samples, into a benign graph prompt tuning process.

D. Theoretical Analysis

Theorem 1 (Universal Graph Prompt Manipulation). *As mentioned in GPF [7], given any frozen pre-trained GNN model f_{pre} and a pre-training task $t \in \mathcal{T}$, any downstream graph $\mathcal{G} = (A, X)$, and any graph prompt generator $g_{\psi_o}(\cdot)$ can be treated as any graph-level transformation $g_{\psi_o} : \mathbb{G} \rightarrow \mathbb{G}$ where $\hat{\mathcal{G}} = g_{\psi_o}(A, X)$, there exist a universal token $\hat{\mathcal{P}}$ that satisfies:*

$$f_{pre}(A, X + \hat{\mathcal{P}}) = f_{pre}(g_{\psi_o}(A, X)) + Err \quad (13)$$

Where g_{ψ_o} can be feature and link transformations, such as modifying the node features, and adding or removing edges, and Err denotes the error bound between the graph prompts and downstream graph regarding pre-trained GNNs for a specific task. Given prompt token \mathcal{P} , token structures \mathcal{E}_Δ , inserting patterns \oplus , and \mathcal{E}_Δ and \oplus are functions of \mathcal{P} and X , such as cosine similarity. Let $\hat{A} = A + \Delta A$, where $\Delta A = A_\Delta + A_\oplus$, which are multiple link transformation operations, thereby following the above theorem. As for graph prompt backdoors, we directly modify the features of graph prompts, which can be seen as multiple feature transformation

operations, therefore, the aforementioned theorem still holds. Please refer to Appendix G for the detailed proof.

V. EXPERIMENTAL VALIDATION

In this section, we conduct empirical experiments based on different types of attacks and trigger generation methods to investigate the following key research questions:

RQ1: How effective/stealthy is Krait for graph backdoors?

RQ2: How does Krait perform under diverse combinations of attack types and trigger generation methods? Can it flexibly adapt to different GNN backbones?

RQ3: What factors can affect the performance of Krait?

RQ4: Can Krait be extended to the black-box setting?

A. Setups

Datasets. We use the same datasets described in Section III.

Model. We set All-in-One [27] as the victim graph prompt tuning model, using the Graph Transformer (GT) [25] as the GNN backbone and GraphCL [44] for pre-training. We consider the multi-class classification setting.

Baselines. To the best of our knowledge, Krait is the first graph prompt backdoor, there is no existing method to compare. Therefore, we use random selection and LNH selection respectively to choose poisoned candidates for each type of attack under diverse trigger generation methods as our baselines.

Implementations. We follow the default parameter settings in All-in-One [27], please refer to more implementation details in Appendix H. Besides, we set adaptation steps as 10, and the trigger size is the same as the graph prompt size, which is 10. We utilize all nodes in each graph dataset instead of sampling a specific number of nodes for training and testing. We 1:1 split the testing samples, half are clean samples and the rest are attached with triggers. And the coefficient $\alpha = 10$. Notably, poisoning rates denote the size of poisoned samples over the node size of the victim label in the training graph, which is much smaller than the whole size of the training graph or victim graph [2], [19]. Since our attack target is mostly the label with the least nodes, the poisoning rates further decrease compared to the existing standards. We report the average results of 5 trials. All experiments are conducted on a 64-bit machine with 4 Nvidia A100 GPUs.

Metrics. For benign models, we use accuracy (ACC), F1 score, and AUC to evaluate the performance of node classification. For graph backdoors, to evaluate attack effectiveness, we employ 1) Attack Success Rate (ASR) to quantify how many trigger-injected samples are misclassified to the target label; 2) average misclassification confidence (AMC) [37] to compute the average confidence score assigned to the target label for the successful graph backdoors. To evaluate attack stealthiness, we use 3) poisoning rate (PR) to represent attack budgets; 4) clean accuracy (CA) to measure the classification accuracy of clean samples after backdoor training; 5) average homophily difference (AHD) to gauge the local-subgraph homophily differences between clean samples and trigger-injected samples.

B. Attack Performance

The performance of benign graph prompt tuning is shown in Table VI in Appendix I. We observe that transfers from different domains are more unstable, and generally lead to worse performance than within-domain transfers, which fits our intuition. Since there exists up to $4 \times 4 \times 3 \times 3$ cases, based on Table VI, we solely pick up 3 representative cases, namely, CiteSeer to Cora (within-domain, positive, small-to-small transfer), Physics to Computers (out-of-domain, relatively negative, and big-to-big transfer) and Physics to CiteSeer (out-of-domain, positive, and big-to-small transfer) to conduct corresponding experiments.

To address RQ1 and RQ2, we compare Krait with baselines under various attack types and trigger generation methods across three transfer cases.

Effectiveness. As shown in Table I, we observe that Krait consistently outperforms the baselines in terms of ASR and AMC, particularly in big-to-big and big-to-small transfers. In almost all attacks, Krait accomplishes higher attack effectiveness compared to the baselines. Notably, solely employing a label non-uniformity homophily strategy without constraints serves as an ablation study, where Krait surpasses or achieves considerable attack performances than random triggers in the most of attack combinations.

Stealthiness. For a fair comparison, we poison 2% of training nodes with the victim label for all experiments. The PRs relative to the entire training graph range from 0.15% to 2% across the three attack types, which are significantly lower than the typical 10% standard for graph backdoor attacks. In one-to-one attacks for small-scale transfers, poisoned samples contain only two nodes; even in more complex scenarios, Krait only poisons 22 nodes but achieves 100% ASR. Besides, compared to the benign classification accuracy of all test samples reported in Table VI, Krait achieves comparable clean accuracy or even surpasses the benign results in all attack types, demonstrating its stealthiness. Regarding statistical properties, the overall homophily changes between clean samples and poisoned nodes are slight (please note that AHD is expressed in percentage), which indicates that Krait effectively evades detection against homophily and node similarity-based defenders [1]. Moreover, Krait utilizes graph prompt tuning itself to generate graph prompts as triggers based on node similarities, making it more difficult to detect by node-similarity defenders. We further discuss the details in Subsection V-E.

Practicability. As shown in Table I, Krait exhibits superior performance with ASRs of 99.56%–100% in all-to-one attacks across all trigger generation methods. The “Invoke” method excels in one-to-one attacks, achieving ASRs between 99.46% and 100%, while the “Interact” method stands out in all-to-all attacks, with ASRs ranging from 6.67% to 31.89%. The relatively lower performance in all-to-all attacks is reasonable since Krait employs a universal trigger, differing from the specific triggers used in the computer vision (CV) domain [3], [9] that require learning distinct triggers for each attack victim and target pair. In real-world applications, attackers can consider their resources, capabilities, preferences, and involved stages to select the most suitable trigger generation method.

Flexibility. We select three combinations of attack types and trigger generation methods, namely, “Invoke” for one-to-one

Transfer (Evaluation) (Metrics)	Method	Model	One-to-One				All-to-One				All-to-All			
			Effectiveness		Stealthiness		Effectiveness		Stealthiness		Effectiveness		Stealthiness	
			ASR	AMC	CA	AHD	ASR	AMC	CA	AHD	ASR	AMC	CA	AHD
Cite2Cora	Invoke	Random	94.22	93.12	86.89	0.18	29.10	91.49	85.74	4.97	4.23	78.19	85.95	9.54
		LNH	95.56	93.20	86.95	0.19	38.68	90.97	85.39	5.02	4.05	77.95	85.63	9.53
		Full	100.00	100.00	86.75	3.02	100.00	100.00	85.83	3.24	6.67	82.60	86.10	10.43
	Interact	Random	42.22	86.68	86.89	0.91	99.91	99.75	85.66	3.65	42.44	93.96	85.74	6.19
		LNH	56.00	89.37	86.95	0.82	95.51	98.86	85.68	3.71	38.38	90.53	85.83	6.19
		Full	62.22	91.77	86.72	1.29	100.00	100.00	85.86	4.05	31.78	89.51	86.13	5.86
	Modify	Random	43.56	85.88	86.90	0.88	100.00	99.84	85.66	3.60	42.61	93.30	85.83	6.38
		LNH	54.67	89.64	86.98	0.93	96.53	98.83	85.74	3.79	38.68	89.56	85.83	6.13
		Full	59.56	91.83	86.69	1.29	100.00	100.00	85.95	4.07	31.89	89.05	86.27	5.80
Phy2Cite	Invoke	Random	83.64	98.76	81.56	9.61	17.14	95.05	81.47	3.13	8.60	94.66	81.11	3.13
		LNH	78.79	97.51	81.78	9.64	17.89	96.40	80.63	3.15	8.46	93.19	79.62	3.31
		Full	100.00	100.00	82.03	11.01	100.00	100.00	79.90	3.97	8.81	92.17	80.34	2.65
	Interact	Random	23.64	65.49	81.53	9.74	97.98	99.81	81.15	3.29	15.87	94.00	80.87	3.22
		LNH	28.79	89.50	80.93	10.03	82.79	98.47	80.00	3.39	14.45	93.84	80.91	3.13
		Full	31.82	93.12	81.84	10.09	99.93	100.00	81.27	4.02	17.29	95.58	79.50	3.13
	Modify	Random	21.21	89.74	81.45	9.70	97.67	99.85	81.30	3.35	14.17	95.01	81.01	3.24
		LNH	32.42	89.45	80.80	9.99	83.12	98.45	80.02	3.41	15.80	94.54	80.36	3.51
		Full	43.33	92.28	81.21	10.02	99.98	100.00	81.03	4.01	16.11	96.25	79.66	3.04
Phy2Comp	Invoke	Random	53.51	95.54	62.21	-5.19	74.42	98.00	62.93	3.08	4.88	93.17	61.02	3.10
		LNH	43.24	94.62	62.25	-5.30	73.56	98.30	60.88	3.12	3.94	93.97	61.67	3.02
		Full	99.46	100.00	63.31	4.73	100.00	100.00	62.74	3.64	25.30	98.31	62.70	3.54
	Interact	Random	25.41	93.02	60.85	-5.25	98.16	99.77	61.20	3.55	5.67	95.16	61.50	2.97
		LNH	24.05	91.85	62.16	-5.27	98.14	99.78	60.28	3.56	7.52	93.37	61.62	2.73
		Full	31.08	91.61	61.70	-5.19	99.82	100.00	63.75	3.90	18.37	99.06	62.64	3.11
	Modify	Random	34.86	94.35	62.15	-5.23	98.76	99.84	60.19	3.51	6.13	96.51	61.17	3.15
		LNH	26.49	92.26	62.28	-5.28	98.26	99.79	60.01	3.51	10.50	95.72	61.76	2.55
		Full	38.11	90.45	61.69	-5.20	99.56	99.98	62.89	3.94	17.75	98.95	59.87	3.16

TABLE I: Performance of Krait under the white-box setting. Cite2Cora: CiteSeer to Cora transfer; Phy2Cite: Physics to CiteSeer transfer; Phy2Comp: Physics to Computers transfer. Random and LNH denote poison node selection strategies, and Full denotes Krait. We bold the best performance under different combinations of attack types and trigger generation methods.

attacks, “Interact” for all-to-one attacks, and “Modify” for all-to-all attacks to report our results in the CiteSeer to Cora transfer case. Except for GT [25], we additionally employ the graph convolutional network (GCN) [13] and graph attention network (GAT) [32] as GNN backbones. Our experimental results show that Krait maintains superior performance in terms of attack effectiveness and stealthiness across different GNN backbones. Specifically, Krait embedded with GT as the backbone excels in most attack combinations. And Krait embedded with different GNN backbones all achieve nearly 100% ASRs in all-to-one attacks that utilize the “Interact” trigger generation method. Please refer to Table VII in Appendix J for more details.

C. Parameter Studies

To answer RQ3, we conduct parameter studies on trigger size, PR, epochs, and constraint coefficient, respectively.

Trigger size. We vary trigger size as [1, 5, 10, 15, 20]. As shown in Figure 7, Krait consistently surpasses the baselines as the trigger size increases. Notably, even with the trigger size set to 1, Krait can still achieve 100% ASRs in one-to-one and all-to-one attacks. However, larger trigger sizes in all-to-all attacks may result in ASR drops. We speculate that since Krait generates a universal trigger for all given attack pairs, it can continuously encode the general malicious knowledge to facilitate graph backdoor attacks before the trigger size reaches an “optimal” threshold. As trigger size grows, Krait may encode redundant information, leading to ASR drops. Sun et al. [27] report similar observations when increasing the size of the prompt token.

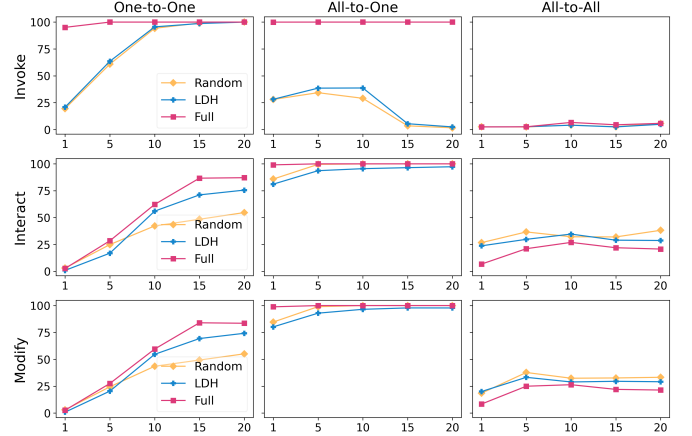


Fig. 7: Impact of trigger size in Krait, x-axis denotes the trigger size while y-axis denotes the ASR.

Poisoning rate. We vary PR as [2, 5, 10, 20, 50]%. From Figure 8, generally, higher PR, higher ASR. Except for all-to-all attacks, the rest of the attacks with diverse trigger generation methods all accomplish 100% ASRs with less than 5% PR.

Training epochs. We vary training epochs as [2, 4, 6, 8, 10]. As shown in Figure 9, generally, larger epochs yield higher ASRs. In one-to-one attacks with the “Invoke” method, only training for 2 epochs with 2 poisoned nodes yields a 100% ASR, and in all-to-one attacks, within 4 training epochs, Krait achieves a 100% ASR with 22 poisoned nodes.

Constraint coefficient. We vary α as [0.1, 0.5, 1, 2, 5]. Inter-

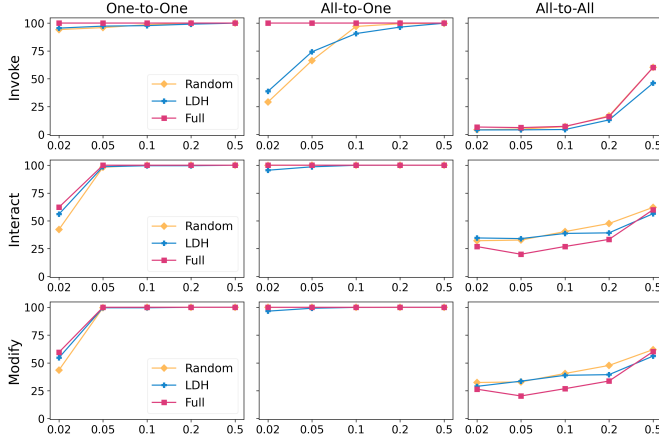


Fig. 8: Impact of poisoning rate in Krait, x-axis denotes the PR while y-axis denotes the ASR.

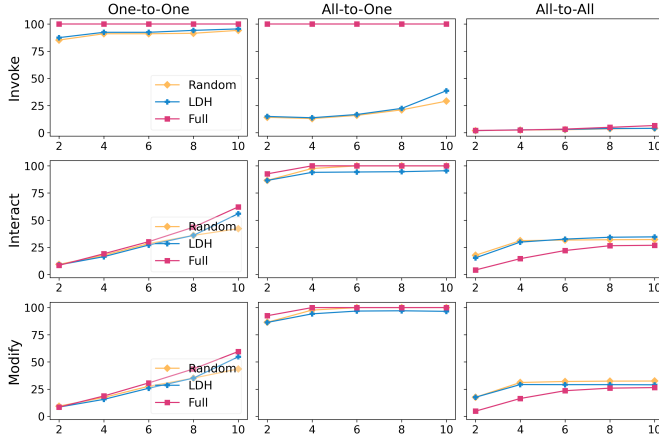


Fig. 9: Impact of training epochs in Krait, x-axis denotes the PR while y-axis denotes the ASR.

estingly, as shown in Figure 10, these three trigger generation methods perform differently for various attack types. In one-to-one attacks, “Invoke” stands out with 100% ASR while “Interact” and “Modify” behave almost the same, where their ASRs first increase and then decrease. Similar patterns are observed in all-to-one attacks, but they all maintain 100% ASR with α less than 2. In all-to-all attacks, the ASRs for “Invoke” monotonically increase, whereas those for “Interact” and “Modify” both decline.

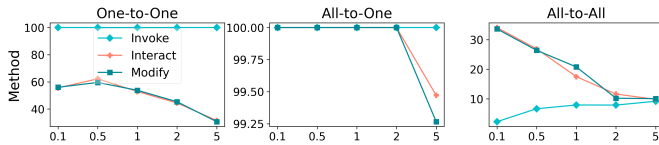


Fig. 10: Impact of the coefficient alpha in Krait, x-axis denotes the alpha while y-axis denotes the ASR.

D. Black-box Setting

We consider a more practical setting where the system or platform does not support custom training and there is no access to intermediate results. To address this black-box setting, Krait can be degraded into the “Invoke” trigger

generation method without the constraint. We leverage All-in-one with different GNN backbones to mimic the open-sourced models in poisoning warm-ups. We set $\alpha \in (0.1, 0.6)$. Due to the harsh setting, we set the PR as 10%, which only poisons 9 nodes in one-to-one attacks and 96 nodes in all-to-one attacks (0.67%, 7% of the whole training graph, respectively), still much lower than the existing standard in graph backdoor attacks. The results are shown in Table II. Under diverse GNN backbones, the black-box Krait still yields comparable performance in terms of attack effectiveness and stealthiness. Krait with the same GT backbone (but with different parameters) achieves superior performance in one-to-one and all-to-one attacks, and Krait with the GCN backbone excels in all-to-all attacks with a 35.95% ASR but it leads to large homophily drops.

E. Discussions

1) Possible Defense Solutions: Given that defense mechanisms against graph backdoor attacks are still in their infancy, we resort to defenses from other graph adversarial attacks and injection-based backdoor detections in different domains to analyze and assess their effectiveness against Krait.

Homophily and node-similarity defenders. Chen et al. [1] propose homophily defenders against graph injection attacks and demonstrate that GNNGuard [46], an acclaimed defense mechanism [45], acts as a homophily defender by pruning suspicious edges if $\text{sim}(X_v, X_u) \leq s_g$, where s_g denotes the minimum similarity for any pair of nodes connected in \mathcal{G} . Nonetheless, GNNGuard becomes ineffective against Krait for the following four reasons: 1) As indicated in Section III, the consistent homophily patterns before and after graph prompt backdoor injections make it more intractable for defenders to identify poisoned nodes; 2) GNNGuard is primarily designed for node classification and cannot be trivially applied to graph prompt backdoor attacks since the latter reformulate node-level tasks to graph-level tasks, complicating the detection of small-scale trigger injection in each ego-network. Meanwhile, as shown in Table I-II, homophily variations between clean samples and poisoned nodes are typically slight; 3) The structure of prompt tokens, which are mainly similarity functions of token features, can be adaptively tuned when crafting poisoned prompts, making them more difficult for homophily defenders to defeat. This challenge likewise extends to node similarity-based detectors mentioned in [51]; 4) Ennadir et al. [4] empirically validate that homophily defenders, i.e., GNNGuard, are 11.78–303.43 times slower than other defense mechanisms. GNN-Jaccard [36], which utilizes Jaccard similarity (only count 0 or 1) to remove suspicious edges if their linked nodes’ similarity scores are close to 0, will lose efficacy since the myriad of graph prompt tuning models [27] employ dimensionality reduction techniques, especially in large-scale graphs with nearly $10k$ node features [24].

Model inspection. Authors in [37] extend NeuralCleanse [33] into graph learning, which computes graph edit distance between triggers and to-be-replaced subgraphs. Krait, however, eliminates the necessity for subgraph replacement, thus restricting the effectiveness of backdoor detection. Even with the allowance, model inspection approaches will attempt to search a specific trigger in every subgraph for $|\mathcal{V}|$ times, which is impractical for large-scale graphs.

Transfer (Evaluation) (Metrics)	Backbone	Model	One-to-One				All-to-One				All-to-All			
			Effectiveness		Stealthiness		Effectiveness		Stealthiness		Effectiveness		Stealthiness	
			ASR	AMC	CA	AHD	ASR	AMC	CA	AHD	ASR	AMC	CA	AHD
Cite2Cora	GCN	Random	34.22	78.65	86.83	9.53	32.13	93.48	85.07	9.63	35.95	95.25	85.48	19.77
		LNH	43.56	85.39	86.81	9.41	44.88	92.50	84.33	9.36	31.45	90.80	86.10	19.65
		Full	41.33	70.16	86.81	14.59	98.41	99.07	84.59	11.45	30.25	91.54	86.16	19.96
	GAT	Random	4.44	35.36	87.10	-1.09	41.00	94.46	84.92	4.16	13.01	76.34	85.60	3.40
		LNH	8.89	45.90	87.04	-1.12	51.07	92.82	84.21	4.18	6.78	71.49	85.83	3.35
		Full	26.67	67.60	86.97	1.79	71.48	94.47	84.33	2.93	6.23	70.94	85.71	2.95
	GT	Random	98.67	96.67	87.00	0.34	97.03	97.35	82.92	4.89	7.02	78.51	85.95	9.72
		LNH	97.78	95.04	86.90	0.30	90.66	95.23	83.12	4.91	4.43	77.81	85.94	9.58
		Full	100.00	100.00	86.95	2.73	100.00	100.00	85.71	3.08	8.81	85.03	85.66	10.32

TABLE II: Performance of Krait under the black-box setting. Cite2Cora: CiteSeer to Cora transfer.

Transfer (Evaluation) (Metrics)	Method	Model	One-to-One				All-to-One				All-to-All			
			Effectiveness		Stealthiness		Effectiveness		Stealthiness		Effectiveness		Stealthiness	
			ASR	AMC	CA	AHD	ASR	AMC	CA	AHD	ASR	AMC	CA	AHD
Cite2Cora	Invoke	GNN-SVD	100.00	100.00	86.77	7.71	100.00	100.00	85.83	6.02	6.90	82.50	86.13	15.72
		Noisy-Fea	100.00	100.00	86.72	3.23	100.00	100.00	85.95	3.54	6.11	80.71	86.07	10.54
		Noisy-Emb	100.00	100.00	86.75	3.02	100.00	100.00	85.83	3.27	6.75	81.74	86.07	10.44
	Interact	GNN-SVD	61.78	91.90	86.69	7.89	100.00	100.00	85.89	7.91	31.01	89.74	86.16	11.29
		Noisy-Fea	64.44	89.72	86.65	1.60	100.00	100.00	86.13	4.32	31.45	90.71	86.16	6.07
		Noisy-Emb	63.56	90.65	86.71	1.29	100.00	100.00	85.86	4.05	31.89	88.47	86.22	5.96
	Modify	GNN-SVD	60.89	90.20	86.69	5.63	100.00	100.00	85.92	6.61	31.60	89.50	86.27	9.83
		Noisy-Fea	64.00	88.27	86.62	1.61	100.00	100.00	86.01	4.35	31.78	88.99	86.24	6.11
		Noisy-Emb	61.78	90.53	86.69	1.29	100.00	100.00	85.92	4.06	31.81	88.61	86.22	5.82

TABLE III: Performance of Krait on GNN-SVD, Noisy-Fea and Noisy-Emb. Cite2Cora: CiteSeer to Cora transfer.

Randomized smoothing. Randomized smoothing [47] is another potential defense mechanism, which samples numerous subgraphs of each ego-network to conduct a majority voting. Nevertheless, defending against graph prompt backdoors is impractical because the sampling operation itself has a complexity of $\mathcal{O}(|V| \cdot \mathcal{C}_s)$, where \mathcal{C}_s is the original complexity of sampling methods. Not to mention the even more time-intensive training for all sampled subgraphs. The total computational costs are prohibitive.

Noise filtering and injection. Another line of defenders manipulates noises to fight against adversarial perturbations. Entezari et al. [5] empirically demonstrate that graph adversarial attacks inject noises into higher ranks in the singular value spectrum. Inspired by this phenomenon, they design GNN-SVD, which employs a low-rank approximation of the adjacency matrix to filter out high-rank noises and reset the remaining values to 1, thus completing the pruning of noisy edges. Inversely, NoisyGNN [4] injects noises from a pre-defined distribution into the node feature/structural space to defend against feature/structural-based adversarial attacks. To align with Krait, we implement GNN-SVD and NoisyGNN for each subgraph. We follow GNN-SVD’s rank recommendation to set rank as 10. As for NoisyGNN, we sample noises from the same Gaussian distribution $\mathcal{N}(0, I)$ with the default scaling parameter as 0.1. We first inject noises into the feature spaces of the prompted subgraphs (marked as Noisy-Fea) as node features play vital roles in graph prompt tuning. Next, since NoisyGNN is designed for node classification tasks and cannot be trivially adapted to graph prompt tuning which involves node-subgraph transformations, we consider a new variant of NoisyGNN (Noisy-Emb) to inject noises into the graph embeddings of the prompted subgraphs. The defense performance is shown in Table III, which indicates these two methods cannot effectively defend against Krait. Interestingly, in some specific cases, such as in the one-to-one attacks with “Modify” as the

trigger generation method, GNN-SVD and the two variants of NoisyGNN actually enhance the attack performance of Krait. We speculate that 1) GNN-SVD may filter out noises that hinder the creation of a solid mapping between triggers and the target label, thus improving attack effectiveness; 2) By adding noises into feature and hidden spaces of poisoned graphs, NoisyGNN reinforces the robustness of Krait, leading to more stable and accurate performance. We leave the exploration of the mechanisms behind this phenomenon for future work.

2) Suggestions for Graph Prompt Protection: Wang et al. [35] indicate that backdoor attacks often yield statistically higher confidence scores of poisoned samples to achieve high ASRs while maintaining relatively low PRs. Although [35] focuses on backdoor attacks in CV, we observe similar patterns of Krait as shown in Table I-II. Additionally, since Krait utilizes graph prompt tuning to craft graph prompts as triggers, the ego-networks of the poisoned candidates typically exhibit larger average degrees compared to the clean samples. The aforementioned evidence and observations inspire us to closely monitor suspicious nodes with unusually higher prediction confidence scores and larger average degrees. However, previous studies in fair graph learning suggest that nodes with larger degrees enjoy more benefits during message-passing processes, resulting in higher confidence scores [16], [31]. Therefore, filtering such suspicious nodes based solely on the above criteria could significantly impair the performance of graph prompt tuning. The same conclusion can be inferred from Figure 11, where the overwhelming majority of clean samples, as well as the poisoned samples, have confidence scores closer to 1. Nevertheless, it is still valuable to monitor nodes with high confidence scores.

Another possible direction is to project suspiciously backdoored embeddings into lower dimensions to identify potential anomalies. To demonstrate whether anomalies exist under 100% ASRs, we choose the “Invoke” trigger genera-

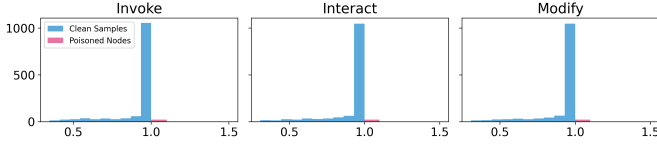


Fig. 11: Confidence score distributions of clean and poisoned samples under three trigger generation methods.

tion method and visualize the node embeddings after one-to-one and all-to-one attacks in Figure 12. We observe that the poisoned samples tend to cluster at the edges of class boundaries. Therefore, comprehensively tracing nodes with high confidence scores and proximity to decision boundaries could be an effective strategy. For more detailed visualizations and analysis, please refer to Appendix K.

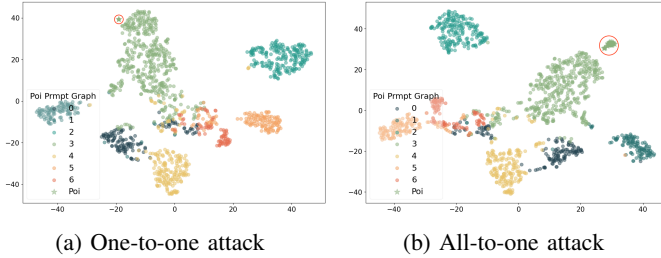


Fig. 12: Backdoored node embedding of “Invoke”, poisoned nodes are marked with red circles.

Moreover, to prevent graph prompt backdoors that utilize “Interact” and “Modify” trigger generation methods, service providers or model/system owners should prohibit the generation of multiple graph prompts for arbitrary node sets. They should also implement rigorous scrutiny and auditing practices to ensure that these prompts and their sources have not been maliciously altered. Moreover, we recommend prioritizing system-automated graph prompts over potentially suspicious hand-crafted prompts, especially when anomalies are detected.

3) Limitations and Future Work: Although our empirical results showcase the attack effectiveness and stealthiness of Krait, we acknowledge several limitations that can pave the way for future work. First, despite the research surge in graph prompt tuning, there is no GPTaaS yet, we anticipate testing the performance of Krait in real-world APIs or platforms. Second, we follow the classical label-flipping strategy to initialize poisoned nodes [2], [37], [39], adapting Krait to the clean-label setting could be a promising direction. Third, since we only evaluate Krait in homophilic graphs, integrating Krait with heterogeneous graph prompts as triggers can further enhance its impacts. Fourth, Krait can be easily extended to multiple graph prompts, which better reflects real-world scenarios. Different attackers can handcraft or hijack different graph prompts at various times, leading to much more severe social impacts. Therefore, this problem should be further highlighted. Finally, it is critical to develop a more reliable defense mechanism against graph prompt backdoors.

VI. RELATED WORK

A. Graph Prompt Tuning

GPPT [26] proposes a graph prompting function to transform each node into a token pair, thereby reformulating down-

stream node-level tasks in line with the pretext. GraphPrompt [17] leverages subgraph similarity to unify pre-training and downstream tasks into a common task template and utilizes learnable prompts to encode the most relevant graph knowledge in a task-specific manner. PRODIGY [10] introduces in-context learning on graphs, employing hand-crafted graph prompts without tunable parameters to represent node, edge, and graph-level tasks. GPF and GPF-plus [7] adopt task-specific tuning to learn a universal feature vector as the prompt, which can be broadly generalized to various pre-training and downstream task adaptations. All-in-one [27] aligns all-level tasks into the graph-level pretext and further treats additional subgraphs as graph prompts, where prompt features can be tuned through meta-learning, and the inner structures and inserting patterns are functions of the prompt features and node features, respectively.

B. Graph Backdoor Attacks

Graph backdoors are largely underexplored. Zhang et al. [47] construct random subgraphs as triggers and then attach these triggers to random nodes. Xi et al. [37] utilize bi-level optimization to adaptively generate triggers that are tailored for specific downstream tasks while implanting these triggers into random nodes. Xu et al. [39] employ explanation-based methods to select the least important nodes as poisoned candidates, randomly altering their features of a predefined size to a fixed value to create feature triggers. Zheng et al. [51] combine motif distributions with subgraph importance to design graph backdoors, empirically demonstrating that using low-importance subgraphs can achieve better attack performance. Dai et al. [2] first identify poisoned samples through node clustering, then leverage bi-level optimization to generate triggers that can survive even after pre-processing defense mechanisms are applied. Zhao et al. [50] develop graph backdoors in the spectral domain by choosing significant feature and frequency bands for injecting trigger signals. Zhang et al. [45] propose the first graph backdoor attack against graph contrastive learning (GCL), which uses discrete optimization to attack possible stages of the GCL pipeline. Lastly, Xu et al. [38] consider one-to-N and N-to-one attacks, which flip labels of randomly sampled nodes and modify their features to specific values. However, N is set to a small number, such as 2 or 4, which cannot cover all node labels needed to launch more advanced one-to-all or all-to-all attacks.

VII. CONCLUSION

In this study, we pioneer the investigation into the inherent vulnerability of graph prompt tuning. We introduce Krait, a novel graph prompt backdoor that utilizes label non-uniformity homophily to effectively select poisoned nodes during the pre-training phase. Additionally, we design three trigger generation methods to treat graph prompts as triggers in distinct scenarios and incorporate a novel centroid similarity-based loss function to enhance the effectiveness and stealthiness of Krait. Our experimental results validate the practicality of Krait across various combinations of attack types, trigger generation methods, and GNN backbones. Moreover, Krait can be successfully extended to the more challenging black-box setting. Finally, we analyze and assess potential countermeasures on Krait, and further address the necessity to develop a reliable defense mechanism against graph prompt backdoor attacks.

REFERENCES

- [1] Y. Chen, H. Yang, Y. Zhang, M. KAILI, T. Liu, B. Han, and J. Cheng, "Understanding and improving graph injection attack by promoting unnoticeability," in *International Conference on Learning Representations*, 2022. [Online]. Available: <https://openreview.net/forum?id=wkMG8cdvh7->
- [2] E. Dai, M. Lin, X. Zhang, and S. Wang, "Unnoticeable backdoor attacks on graph neural networks," in *Proceedings of the ACM Web Conference 2023*, ser. WWW '23. New York, NY, USA: Association for Computing Machinery, 2023, p. 2263–2273. [Online]. Available: <https://doi.org/10.1145/3543507.3583392>
- [3] K. D. Doan, Y. Lao, and P. Li, "Marksman backdoor: backdoor attacks with arbitrary target class," in *Proceedings of the 36th International Conference on Neural Information Processing Systems*, ser. NIPS '22. Red Hook, NY, USA: Curran Associates Inc., 2024.
- [4] S. Ennadir, Y. Abbahaddou, J. F. Lutzeyer, M. Vazirgiannis, and H. Boström, "A simple and yet fairly effective defense for graph neural networks," *Proceedings of the AAAI Conference on Artificial Intelligence*, vol. 38, no. 19, pp. 21 063–21 071, Mar. 2024. [Online]. Available: <https://ojs.aaai.org/index.php/AAAI/article/view/30098>
- [5] N. Entezari, S. A. Al-Sayouri, A. Darvishzadeh, and E. E. Papalexakis, "All you need is low (rank): Defending against adversarial attacks on graphs," in *Proceedings of the 13th International Conference on Web Search and Data Mining*, ser. WSDM '20. New York, NY, USA: Association for Computing Machinery, 2020, p. 169–177. [Online]. Available: <https://doi.org/10.1145/3336191.3371789>
- [6] W. Fan, Y. Ma, Q. Li, Y. He, E. Zhao, J. Tang, and D. Yin, "Graph neural networks for social recommendation," in *The World Wide Web Conference*, ser. WWW '19. New York, NY, USA: Association for Computing Machinery, 2019, p. 417–426. [Online]. Available: <https://doi.org/10.1145/3308558.3313488>
- [7] T. Fang, Y. Zhang, Y. YANG, C. Wang, and L. Chen, "Universal prompt tuning for graph neural networks," in *Advances in Neural Information Processing Systems*, A. Oh, T. Neumann, A. Globerson, K. Saenko, M. Hardt, and S. Levine, Eds., vol. 36. Curran Associates, Inc., 2023, pp. 52 464–52 489. [Online]. Available: https://proceedings.neurips.cc/paper_files/paper/2023/file/a4a1ee071ce0fe63b83bce507c9dc4d7-Paper-Conference.pdf
- [8] X. Gong, Y. Chen, W. Yang, H. Huang, and Q. Wang, "B3: Backdoor attacks against black-box machine learning models," *ACM Trans. Priv. Secur.*, vol. 26, no. 4, aug 2023. [Online]. Available: <https://doi.org/10.1145/3605212>
- [9] T. Gu, K. Liu, B. Dolan-Gavitt, and S. Garg, "Badnets: Evaluating backdooring attacks on deep neural networks," *IEEE Access*, vol. 7, pp. 47 230–47 244, 2019.
- [10] Q. Huang, H. Ren, P. Chen, G. Kržmanc, D. Zeng, P. Liang, and J. Leskovec, "PRODIGY: Enabling in-context learning over graphs," in *Thirty-seventh Conference on Neural Information Processing Systems*, 2023. [Online]. Available: <https://openreview.net/forum?id=pLwYhNNnoR>
- [11] F. Ji, S. H. Lee, H. Meng, K. Zhao, J. Yang, and W. P. Tay, "Leveraging label non-uniformity for node classification in graph neural networks," in *Proceedings of the 40th International Conference on Machine Learning*, ser. ICML'23. JMLR.org, 2023.
- [12] B. Jin, G. Liu, C. Han, M. Jiang, H. Ji, and J. Han, "Large language models on graphs: A comprehensive survey," 2024.
- [13] T. N. Kipf and M. Welling, "Semi-supervised classification with graph convolutional networks," in *International Conference on Learning Representations*, 2017. [Online]. Available: <https://openreview.net/forum?id=SJU4ayYgl>
- [14] L. Li, Y. Zhang, and L. Chen, "Prompt distillation for efficient llm-based recommendation," in *Proceedings of the 32nd ACM International Conference on Information and Knowledge Management*, ser. CIKM '23. New York, NY, USA: Association for Computing Machinery, 2023, p. 1348–1357. [Online]. Available: <https://doi.org/10.1145/3583780.3615017>
- [15] M. M. Li, K. Huang, and M. Zitnik, "Graph representation learning in biomedicine and healthcare," *Nature Biomedical Engineering*, vol. 6, pp. 1353 – 1369, 2022. [Online]. Available: <https://api.semanticscholar.org/CorpusID:253245343>
- [16] Z. Liu, T.-K. Nguyen, and Y. Fang, "On generalized degree fairness in graph neural networks," in *Proceedings of the Thirty-Seventh AAAI Conference on Artificial Intelligence and Thirty-Fifth Conference on Innovative Applications of Artificial Intelligence and Thirteenth Symposium on Educational Advances in Artificial Intelligence*, ser. AAAI'23/IAAI'23/EAAI'23. AAAI Press, 2023. [Online]. Available: <https://doi.org/10.1609/aaai.v37i4.25574>
- [17] Z. Liu, X. Yu, Y. Fang, and X. Zhang, "Graphprompt: Unifying pre-training and downstream tasks for graph neural networks," in *Proceedings of the ACM Web Conference 2023*, ser. WWW '23. New York, NY, USA: Association for Computing Machinery, 2023, p. 417–428. [Online]. Available: <https://doi.org/10.1145/3543507.3583386>
- [18] S. Luan, C. Hua, M. Xu, Q. Lu, J. Zhu, X.-W. Chang, J. Fu, J. Leskovec, and D. Precup, "When do graph neural networks help with node classification? investigating the homophily principle on node distinguishability," in *Thirty-seventh Conference on Neural Information Processing Systems*, 2023. [Online]. Available: <https://openreview.net/forum?id=kJmYu3TiZz>
- [19] P. Lv, C. Yue, R. Liang, Y. Yang, S. Zhang, H. Ma, and K. Chen, "A data-free backdoor injection approach in neural networks," in *32nd USENIX Security Symposium (USENIX Security 23)*. Anaheim, CA: USENIX Association, Aug. 2023, pp. 2671–2688. [Online]. Available: <https://www.usenix.org/conference/usenixsecurity23/presentation/lv>
- [20] Y. Ma, X. Liu, N. Shah, and J. Tang, "Is homophily a necessity for graph neural networks?" in *International Conference on Learning Representations*, 2022. [Online]. Available: <https://openreview.net/forum?id=ucASPPD9GKN>
- [21] Y. Ma, Y. Tian, N. Moniz, and N. V. Chawla, "Class-imbalanced learning on graphs: A survey," 2023.
- [22] D. Morgenstern and G. F. King, "The venom optimization hypothesis revisited," *Toxicon*, vol. 63, pp. 120–128, 2013. [Online]. Available: <https://www.sciencedirect.com/science/article/pii/S0041010112008173>
- [23] L. Peng, S. Cai, Z. Wu, H. Shang, X. Zhu, and X. Li, "Mmgpl: Multimodal medical data analysis with graph prompt learning," 2023.
- [24] O. Shchur, M. Mumme, A. Bojchevski, and S. Günnemann, "Pitfalls of graph neural network evaluation," 2019.
- [25] Y. Shi, Z. Huang, S. Feng, H. Zhong, W. Wang, and Y. Sun, "Masked label prediction: Unified message passing model for semi-supervised classification," in *Proceedings of the Thirtieth International Joint Conference on Artificial Intelligence, IJCAI-21*, Z.-H. Zhou, Ed. International Joint Conferences on Artificial Intelligence Organization, 8 2021, pp. 1548–1554, main Track. [Online]. Available: <https://doi.org/10.24963/ijcai.2021/214>
- [26] M. Sun, K. Zhou, X. He, Y. Wang, and X. Wang, "Gppt: Graph pre-training and prompt tuning to generalize graph neural networks," in *Proceedings of the 28th ACM SIGKDD Conference on Knowledge Discovery and Data Mining*, ser. KDD '22. New York, NY, USA: Association for Computing Machinery, 2022, p. 1717–1727. [Online]. Available: <https://doi.org/10.1145/3534678.3539249>

- [27] X. Sun, H. Cheng, J. Li, B. Liu, and J. Guan, "All in one: Multi-task prompting for graph neural networks," in *Proceedings of the 29th ACM SIGKDD Conference on Knowledge Discovery and Data Mining*, ser. KDD '23. New York, NY, USA: Association for Computing Machinery, 2023, p. 2120–2131. [Online]. Available: <https://doi.org/10.1145/3580305.3599256>
- [28] X. Sun, J. Zhang, X. Wu, H. Cheng, Y. Xiong, and J. Li, "Graph prompt learning: A comprehensive survey and beyond," 2023.
- [29] Z. Tan, R. Guo, K. Ding, and H. Liu, "Virtual node tuning for few-shot node classification," in *Proceedings of the 29th ACM SIGKDD Conference on Knowledge Discovery and Data Mining*, ser. KDD '23. New York, NY, USA: Association for Computing Machinery, 2023, p. 2177–2188. [Online]. Available: <https://doi.org/10.1145/3580305.3599541>
- [30] J. Tang, J. Li, Z. Gao, and J. Li, "Rethinking graph neural networks for anomaly detection," in *International Conference on Machine Learning*, 2022.
- [31] X. Tang, H. Yao, Y. Sun, Y. Wang, J. Tang, C. Aggarwal, P. Mitra, and S. Wang, "Investigating and mitigating degree-related biases in graph convolutional networks," in *Proceedings of the 29th ACM International Conference on Information & Knowledge Management*, ser. CIKM '20. New York, NY, USA: Association for Computing Machinery, 2020, p. 1435–1444. [Online]. Available: <https://doi.org/10.1145/3340531.3411872>
- [32] P. Veličković, G. Cucurull, A. Casanova, A. Romero, P. Liò, and Y. Bengio, "Graph attention networks," in *International Conference on Learning Representations*, 2018. [Online]. Available: <https://openreview.net/forum?id=rJXMPikCZ>
- [33] B. Wang, Y. Yao, S. Shan, H. Li, B. Viswanath, H. Zheng, and B. Y. Zhao, "Neural cleanse: Identifying and mitigating backdoor attacks in neural networks," in *2019 IEEE Symposium on Security and Privacy (SP)*, 2019, pp. 707–723.
- [34] K. Wang, H. Deng, Y. Xu, Z. Liu, and Y. Fang, "Multi-target label backdoor attacks on graph neural networks," *Pattern Recognition*, vol. 152, p. 110449, 2024. [Online]. Available: <https://www.sciencedirect.com/science/article/pii/S0031320324002000>
- [35] T. Wang, Y. Yao, F. Xu, M. Xu, S. An, and T. Wang, "Inspecting prediction confidence for detecting black-box backdoor attacks," *Proceedings of the AAAI Conference on Artificial Intelligence*, vol. 38, no. 1, pp. 274–282, Mar. 2024. [Online]. Available: <https://ojs.aaai.org/index.php/AAAI/article/view/27780>
- [36] H. Wu, C. Wang, Y. Tyshetskiy, A. Docherty, K. Lu, and L. Zhu, "Adversarial examples for graph data: Deep insights into attack and defense," in *Proceedings of the Twenty-Eighth International Joint Conference on Artificial Intelligence, IJCAI-19*. International Joint Conferences on Artificial Intelligence Organization, 7 2019, pp. 4816–4823. [Online]. Available: <https://doi.org/10.24963/ijcai.2019/669>
- [37] Z. Xi, R. Pang, S. Ji, and T. Wang, "Graph backdoor," in *30th {USENIX} Security Symposium ({USENIX} Security 21)*, 2021.
- [38] J. Xu and S. Picek, "Poster: Multi-target & multi-trigger backdoor attacks on graph neural networks," in *Proceedings of the 2023 ACM SIGSAC Conference on Computer and Communications Security*, ser. CCS '23. New York, NY, USA: Association for Computing Machinery, 2023, p. 3570–3572. [Online]. Available: <https://doi.org/10.1145/3576915.3624387>
- [39] J. Xu, M. J. Xue, and S. Picek, "Explainability-based backdoor attacks against graph neural networks," in *Proceedings of the 3rd ACM Workshop on Wireless Security and Machine Learning*, ser. WiseML '21. New York, NY, USA: Association for Computing Machinery, 2021, p. 31–36. [Online]. Available: <https://doi.org/10.1145/3468218.3469046>
- [40] S. Yang, B. G. Doan, P. Montague, O. De Vel, T. Abraham, S. Camtepe, D. C. Ranasinghe, and S. S. Kanhere, "Transferable graph backdoor attack," in *Proceedings of the 25th International Symposium on Research in Attacks, Intrusions and Defenses*, ser. RAID '22. New York, NY, USA: Association for Computing Machinery, 2022, p. 321–332. [Online]. Available: <https://doi.org/10.1145/3545948.3545976>
- [41] Z. Yang, W. W. Cohen, and R. Salakhutdinov, "Revisiting semi-supervised learning with graph embeddings," in *Proceedings of the 33rd International Conference on Machine Learning*, ser. ICML '16. JMLR.org, 2016, p. 40–48.
- [42] B. Yao, G. Chen, R. Zou, Y. Lu, J. Li, S. Zhang, Y. Sang, S. Liu, J. Hendler, and D. Wang, "More samples or more prompts? exploring effective in-context sampling for llm few-shot prompt engineering," 2024.
- [43] Z. Yi, I. Ounis, and C. MacDonald, "Contrastive graph prompt-tuning for cross-domain recommendation," *ACM Trans. Inf. Syst.*, vol. 42, no. 2, dec 2023. [Online]. Available: <https://doi.org/10.1145/3618298>
- [44] Y. You, T. Chen, Y. Sui, T. Chen, Z. Wang, and Y. Shen, "Graph contrastive learning with augmentations," in *Proceedings of the 34th International Conference on Neural Information Processing Systems*, ser. NIPS '20. Red Hook, NY, USA: Curran Associates Inc., 2020.
- [45] H. Zhang, J. Chen, L. Lin, J. Jia, and D. Wu, "Graph contrastive backdoor attacks," in *Proceedings of the 40th International Conference on Machine Learning*, ser. Proceedings of Machine Learning Research, A. Krause, E. Brunskill, K. Cho, B. Engelhardt, S. Sabato, and J. Scarlett, Eds., vol. 202. PMLR, 23–29 Jul 2023, pp. 40 888–40 910. [Online]. Available: <https://proceedings.mlr.press/v202/zhang23e.html>
- [46] X. Zhang and M. Zitnik, "Gnn-guard: Defending graph neural networks against adversarial attacks," in *NeurIPS*, 2020.
- [47] Z. Zhang, J. Jia, B. Wang, and N. Z. Gong, "Backdoor attacks to graph neural networks," in *Proceedings of the 26th ACM Symposium on Access Control Models and Technologies*, ser. SACMAT '21. New York, NY, USA: Association for Computing Machinery, 2021, p. 15–26. [Online]. Available: <https://doi.org/10.1145/3450569.3463560>
- [48] S. Zhao, M. Jia, L. A. Tuan, F. Pan, and J. Wen, "Universal vulnerabilities in large language models: Backdoor attacks for in-context learning," 2024.
- [49] S. Zhao, J. Wen, A. Luu, J. Zhao, and J. Fu, "Prompt as triggers for backdoor attack: Examining the vulnerability in language models," in *Proceedings of the 2023 Conference on Empirical Methods in Natural Language Processing*, H. Bouamor, J. Pino, and K. Bali, Eds. Singapore: Association for Computational Linguistics, Dec. 2023, pp. 12 303–12 317. [Online]. Available: <https://aclanthology.org/2023.emnlp-main.757>
- [50] X. Zhao, H. Wu, and X. Zhang, "Effective backdoor attack on graph neural networks in spectral domain," *IEEE Internet of Things Journal*, vol. 11, no. 7, pp. 12 102–12 114, 2024.
- [51] H. Zheng, H. Xiong, J. Chen, H. Ma, and G. Huang, "Motif-backdoor: Rethinking the backdoor attack on graph neural networks via motifs," *IEEE Transactions on Computational Social Systems*, vol. 11, no. 2, pp. 2479–2493, 2024.

APPENDIX

A. Dataset Statistics

We leverage 4 real-world graph datasets that are extensively evaluated for node classification tasks, including 1) Cora and CiteSeer [41], where each node denotes a document with a bag-of-words representation, and each edge represents a citation relationship; 2) Physics [24], where each node represents an author, the node feature contains paper keywords for each author's papers and each edge indicates authors'

collaborations; 3) Computers [24], where each node represents a product, each node feature is product review encoded by a bag-of-words model, and each edge indicates that two products are frequently purchased together. The detailed graph statistics are shown in Table IV.

Datasets	Nodes	Edges	Features	Labels	Avg. Deg	Homo.(%)
Cora	2,708	10,556	1,433	7	2.65	81.40
CiteSeer	3,327	9,104	3,703	6	2.74	70.62
Physics	34,493	495,924	8,415	5	14.38	91.53
Computers	13,752	491,722	767	10	35.76	78.53

TABLE IV: Detailed statistics of four graph datasets.

B. Benign and attack performance of graph prompt tuning

Source\Target (Metrics)	Cora				CiteSeer			
	ACC	F1	AUC	ASR	ACC	F1	AUC	ASR
Cora	81.03	69.55	95.64	100.00	78.74	68.38	91.08	99.72
CiteSeer	71.25	53.24	89.52	100.00	81.86	80.83	87.85	100.00
Physics	69.04	63.65	88.14	100.00	79.94	78.76	90.35	99.72
Computers	30.15	6.62	51.88	100.00	70.03	62.58	88.51	100.00

TABLE V: Performance of benign and trigger-injected graph prompt tuning, We bold the best performance.

C. Node-centric Homophily

The local-subgraph and global-view homophily distributions of the whole training graph in the CiteSeer to Cora transfer are shown in Figure 13. Since there exist eight transfer cases, we only present the homophily distributions of the poisoned samples with Cora as the target domain in Figures 14-16. As depicted in Section III, except for the negative transfer from Computers to Cora, the rest of transfers exhibit the consistent patterns.

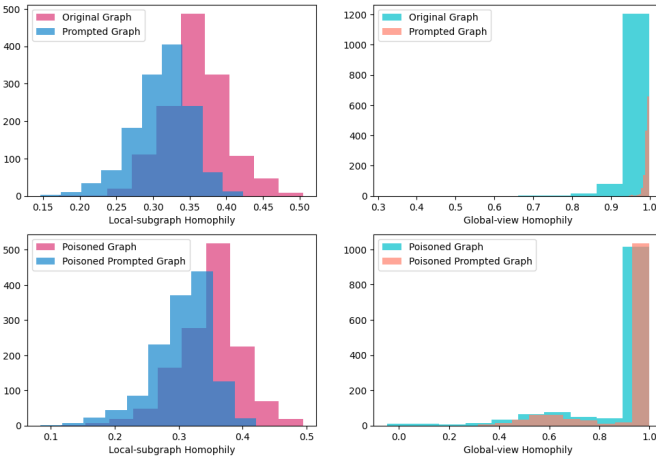


Fig. 13: Local-subgraph(LHS) and global-view(RHS) homophily distributions of the whole training graph in the CiteSeer to Cora transfer.

D. Centroid Similarity

Since there exist eight transfer cases, we only present the centroid alignment, misalignment and difference distributions

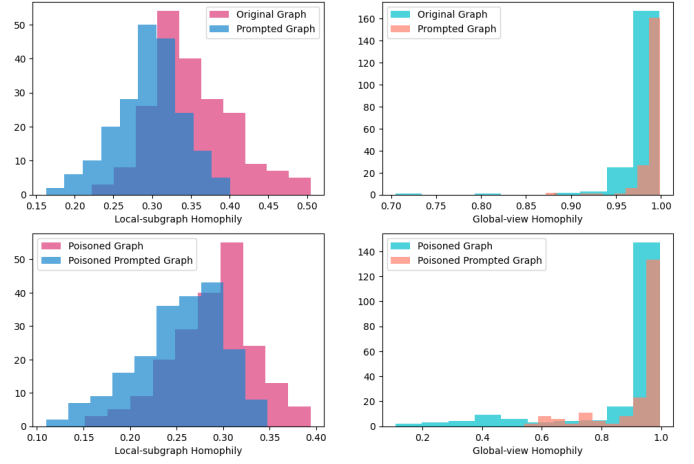


Fig. 14: Local-subgraph(LHS) and global-view(RHS) homophily distributions of poisoned nodes in the Cora to Cora transfer.

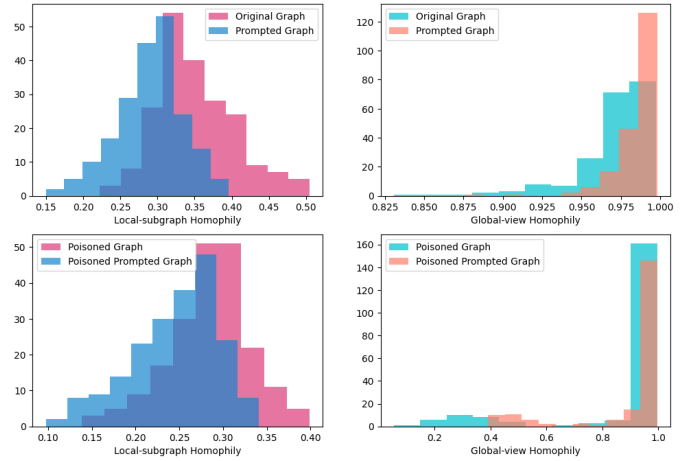


Fig. 15: Local-subgraph(LHS) and global-view(RHS) homophily distributions of poisoned nodes in the Physics to Cora transfer.

of the poisoned samples with Cora as the target domain in Figures 17-19. As depicted in Section III, except for the negative transfer from Computers to Cora, the rest of transfers render the consistent patterns.

E. Embedding Space Visualization

Similarly, we only present the node embedding visualization with Cora as the target domain in Figures 20-22. As depicted in Section III, except for the negative transfer from Computers to Cora, the rest of transfers render the consistent patterns.

F. Algorithms

In this section, we present the overview algorithm of poisoned candidate selection based on different attack types and how to train Krait under diverse trigger generation methods.

1) Algorithm 1 - Poisoned Candidate Selection:

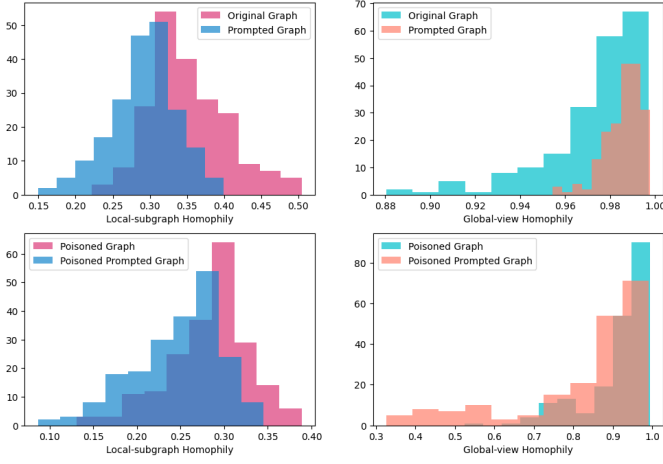


Fig. 16: Local-subgraph(LHS) and global-view(RHS) homophily distributions of poisoned nodes in the Computers to C-ora transfer.

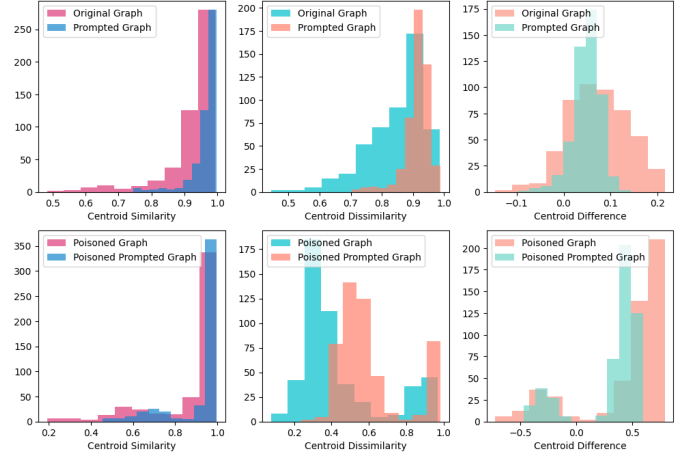


Fig. 18: Centroid alignment(LHS), misalignment(Center) and difference(RHS) distributions of poisoned nodes in the Physics to Cora transfer.

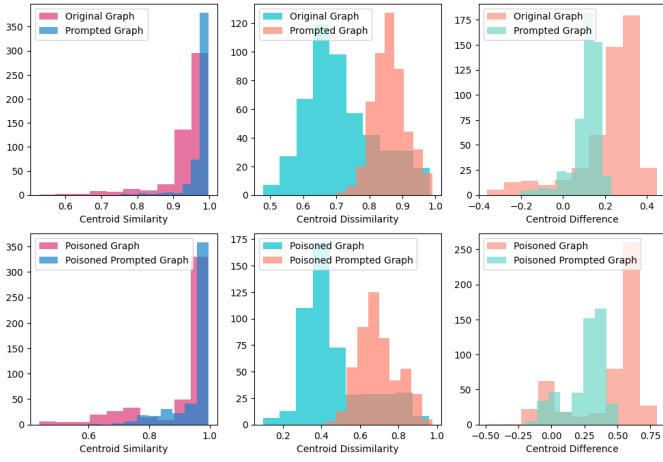


Fig. 17: Centroid alignment(LHS), misalignment(Center) and difference(RHS) distributions of poisoned nodes in the Cora to Cora transfer.

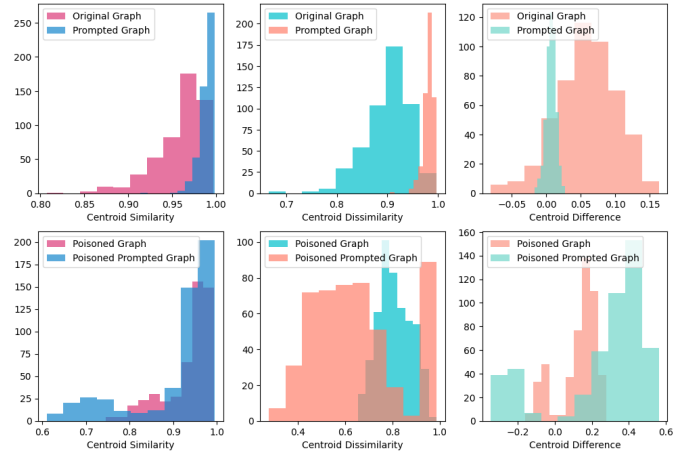


Fig. 19: Centroid alignment(LHS), misalignment(Center) and difference(RHS) distributions of poisoned nodes in the Computers to Cora transfer.

2) Algorithm 2 - Krait:

G. Theoretical Proofs

Theorem 2 (Multiple Graph Prompt Manipulation). *Given any frozen pre-trained GNN model f_{pre} and a pre-training task $t \in \mathcal{T}$, any downstream graph $\mathcal{G} = (A, X)$, and any graph prompt generator $g_\psi(g_{\psi_1}, \dots, g_{\psi_m})$ can be treated as a series of graph-level transformation $g_\psi : \mathbb{G} \rightarrow \mathbb{G}$ where $\hat{\mathcal{G}} = g_\psi(A, X)$, and m is the maximized graph edit distance, there exist a universal token \hat{P} that satisfies:*

$$f_{pre}(A, X + \hat{P}) = f_{pre}(g_\psi(A, X)) + Err \quad (14)$$

Proof: Without loss of generality, we consider 2 graph-level transformations $g_{psi} = (g_{\psi_1}, g_{\psi_2})$, where g_{ψ_1} is the feature transformation and g_{ψ_2} is the link transformation, then based on Propositions 3–5 in [7], there exist a universal token

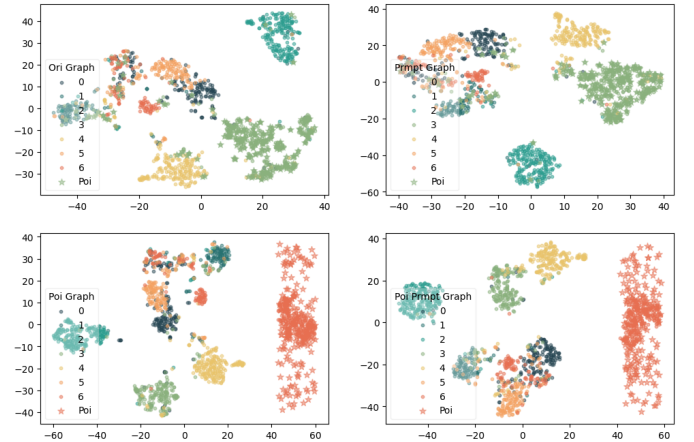


Fig. 20: Node embeddings in the Cora to Cora transfer.

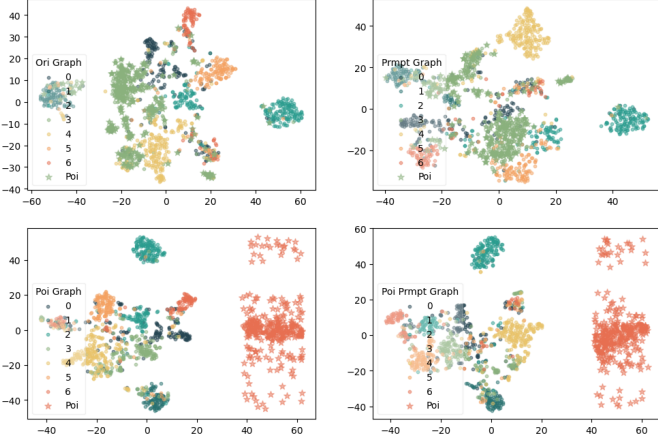


Fig. 21: Node embeddings in the Physics to Cora transfer.

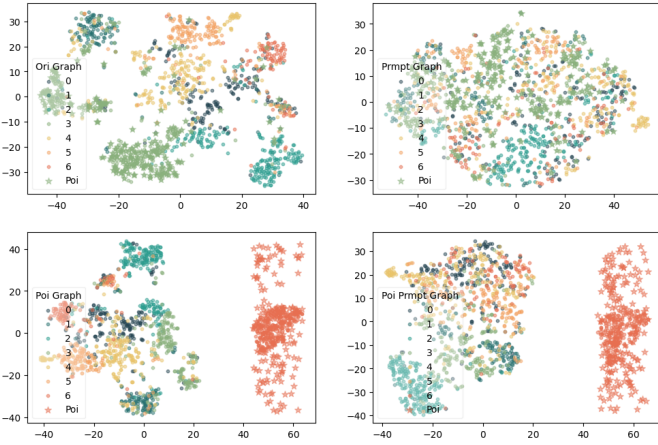


Fig. 22: Node embeddings in the Computers to Cora transfer.

$\hat{\mathcal{P}}_1$ that satisfies:

$$f_{pre}^*(A, X + \hat{\mathcal{P}}_1) \approx f_{pre}^*(g_{\psi_1}(A, X)) \quad (15)$$

and likewise a universal token $\hat{\mathcal{P}}_2$ that satisfies:

$$f_{pre}^*(A, X + \hat{\mathcal{P}}_2) \approx f_{pre}^*(g_{\psi_2}(A, X)) \quad (16)$$

When $\hat{\mathcal{P}} = \hat{\mathcal{P}}_1 + \hat{\mathcal{P}}_2$, then the following equation holds:

$$f_{pre}^*(A, X + \hat{\mathcal{P}}) \approx f_{pre}^*(g_{\psi_1}(g_{\psi_2}(A, X))) \quad (17)$$

■

This 2-step transformation can be easily generalized into multiple steps by repeating the above procedures multiple times, thereby completing the proof.

H. Implementation Details

We follow the default settings of All-in-One [27]. We set the number of graph neural layers as 2 with a hidden dimension of 100 and leverage SVD (Singular Value Decomposition) to reduce the initial features to 100 dimensions. For pre-training, the learning rate is set to 0.01, weight decay is $1e-4$, and epoch is 100. For prompt tuning, the cross-pruning rate is set to

Algorithm 1 Poisoned Candidate Selection

Require: Training graph \mathcal{G}_{train} , poisoning rate p , pre-defined degree threshold d_{pre} , ground-truth label Y , current label Y_c , target label Y_t , attack type m , index searching function $idx(\cdot)$, choosing top k function $topk(\cdot)$, ranking function $rnk(\cdot)$

Ensure: Poisoned candidates \mathcal{B}

```

1: function ONE2ONE( $\mathcal{G}_{train}, p, d_{pre}, Y_c$ )
2:   for each  $i \in \mathcal{G}_{train}$  do
3:     if  $Y_i = Y_c$  &  $d(i) \leq d_{pre}$  then
4:        $\mathcal{G}_{cur} \leftarrow \mathcal{G}_{train}$ 
5:     Compute  $LNH_{cur}$  as in Equation 10
6:      $r_{cur} = rnk(LNH_{cur})$ 
7:      $b = topk(r_{cur}), k = p \times |\mathcal{V}_{cur}|$ 
8:      $\mathcal{B} = idx(b)$ 
9:   return  $\mathcal{B}$ 
10: if  $m = \text{one-to-one}$  then
11:   Implement ONE2ONE, return  $\mathcal{B}$ 
12:    $Y_B \leftarrow Y_t$ 
13:    $\mathcal{G}_{l_{train}} \leftarrow \mathcal{G}_{train}$ 
14: else if  $m = \text{all-to-one}$  then
15:    $\mathcal{B} \leftarrow \emptyset$ 
16:   for  $j \in |Y|$  do
17:     if  $j \neq Y_t$  then
18:        $\mathcal{B}_j = ONE2ONE(\mathcal{G}_{train}, p, d_{pre}, j)$ 
19:        $\mathcal{B} = \mathcal{B} \cup \mathcal{B}_j$ 
20:    $Y_B \leftarrow Y_t$ 
21:    $\mathcal{G}_{l_{train}} \leftarrow \mathcal{G}_{train}$ 
22: else if  $m = \text{all-to-all}$  then
23:    $\mathcal{B} \leftarrow \emptyset$ 
24:   for  $j \in |Y|$  do
25:      $\mathcal{B}_j = ONE2ONE(\mathcal{G}_{train}, p, d_{pre}, j)$ 
26:      $\mathcal{B} = \mathcal{B} \cup \mathcal{B}_j$ 
27:      $Y_t \leftarrow (j + 1) \bmod |Y|$ 
28:      $Y_{B_j} \leftarrow Y_t$ 
29:    $\mathcal{G}_{l_{train}} \leftarrow \mathcal{G}_{train}$ 
30: else
31:   break
32: return  $\mathcal{B}, \mathcal{G}_{l_{train}}$ 

```

0.1 and the inner-pruning rate is 0.3. We utilize cross-entropy loss throughout our experiments. And batch size is 10. For more inner parameters, please refer to All-in-One’s GitHub repository: <https://github.com/sheldonresearch/ProG/tree/main>.

I. Benign Performance of Graph Prompt Tuning

J. Flexibility of Krait

K. Backdoored Node Embedding Visualization

1) *Prompted Node Embedding with the “Interact” Injection:* As shown in Figure 23, the projection of poisoned samples exhibits similar patterns as in Figure 12, where these samples are at the edge of class boundaries, regardless of attack types.

2) *Prompted Node Embedding with the “Modify” Injection:* As shown in Figure 24, similar to the “Invoke” and “Interact” trigger generation methods, poisoned samples are at the edge of class boundaries, regardless of attack types.

Src\Tar	Cora			CiteSeer			Physics			Computers		
(Metrics)	ACC	F1	AUC	ACC	F1	AUC	ACC	F1	AUC	ACC	F1	AUC
Cora	82.22	73.97	95.98	80.76	73.99	91.77	87.58	82.51	94.20	56.46	25.62	66.18
CiteSeer	86.85	84.96	96.63	83.07	82.37	89.12	82.70	64.67	85.91	50.02	17.48	62.22
Physics	72.04	59.68	88.85	80.32	77.46	91.54	79.94	67.11	87.59	61.92	28.34	72.66
Computers	47.10	25.25	67.63	54.50	40.01	78.63	79.73	59.26	81.14	47.44	17.64	60.79

TABLE VI: Performance of benign graph prompt tuning. The row/column denotes the source/target domains, respectively. We bold the best performance in each transfer case.

Transfer	Backbone	Model	One-to-One(Invoke)				All-to-One(Interact)				All-to-All(Modify)			
(Evaluation)			Effectiveness		Stealthiness		Effectiveness		Stealthiness		Effectiveness		Stealthiness	
(Metrics)			ASR	AMC	CA	AHD	ASR	AMC	CA	AHD	ASR	AMC	CA	AHD
Cite2Cora	GCN	Random	16.00	82.91	87.70	6.79	98.24	99.12	86.57	5.25	31.25	93.77	86.75	4.58
		LNH	30.67	84.36	87.73	6.62	98.59	99.10	86.77	5.72	27.75	90.12	86.54	3.94
		Full	86.89	95.75	87.73	9.94	94.13	98.70	86.45	6.63	26.81	94.49	86.36	4.13
	GAT	Random	60.44	93.32	69.52	0.59	99.38	99.97	66.33	4.94	16.42	91.15	68.13	5.06
		LNH	66.67	94.73	71.67	0.63	99.21	99.95	67.30	5.16	16.24	93.32	67.72	5.52
		Full	100.00	99.80	71.91	3.34	100.00	100.00	68.57	5.44	13.63	89.35	66.22	4.96
	GT	Random	94.22	93.12	86.89	0.18	99.91	99.75	85.66	3.65	42.61	93.30	85.83	6.38
		LNH	95.56	93.20	86.95	0.19	95.51	98.86	85.68	3.71	38.68	89.56	85.83	6.13
		Full	100.00	100.00	86.75	3.02	100.00	100.00	85.86	4.05	31.89	89.05	86.27	5.80

TABLE VII: Performance of Krait under different GNN backbones. Cite2Cora: CiteSeer to Cora transfer.

Algorithm 2 Krait

Require: Training graph \mathcal{G}_{train} , poisoning rate p , pre-defined degree threshold d_{pre} , ground-truth label Y , current label Y_c , target label Y_t , attack type m , trigger generation method ρ , poisoned warm-up candidates \mathcal{G}_P , default parameters dft , training process $opt(\cdot)$

Ensure: Backdoored graph prompt tuning model f'_{prm}

```

1: Implement Algorithm 1
2: if  $\rho = \text{invoke}$  then
3:   Initialize  $g_\psi$ 
4:   Implement  $f_{prm}(dft, \mathcal{G}_P)$ , return poisoned  $g'_\psi$ 
5:    $\mathcal{G}'_{train} \leftarrow g'_\psi(\mathcal{G}_{train})$ 
6:   for  $i \in (1, epochs)$  do
7:      $f'_{prm} = opt(dft, f_{prm}, g_\psi, \mathcal{G}'_{train}, \mathcal{L}_{bkd})$ 
8: else if  $m = \text{interact}$  then
9:   Initialize  $g_\psi, g'_\psi$ 
10:  for  $i \in (1, epochs)$  do
11:     $\mathcal{G}'_{train} \leftarrow g'_\psi(\mathcal{G}_{train})$ 
12:     $\mathcal{G}'_{train} \leftarrow g'_\psi(\mathcal{G}'_{train})$ 
13:     $f'_{prm} = opt(dft, f_{prm}, g_\psi, g'_\psi, \mathcal{G}'_{train}, \mathcal{L}_{bkd})$ 
14: else if  $m = \text{modify}$  then
15:   Initialize  $g_\psi, g'_\psi$ 
16:   for  $i \in (1, epochs)$  do
17:      $\mathcal{G}'_{train} \leftarrow g_\psi(\mathcal{G}'_{train})$ 
18:      $\mathcal{G}'_{train} \leftarrow g'_\psi(\mathcal{G}'_{train})$ 
19:      $f'_{prm} = opt(dft, f_{prm}, g_\psi, g'_\psi, \mathcal{G}'_{train}, \mathcal{L}_{bkd})$ 
20: else
21:   break
return  $f'_{prm}$ 

```

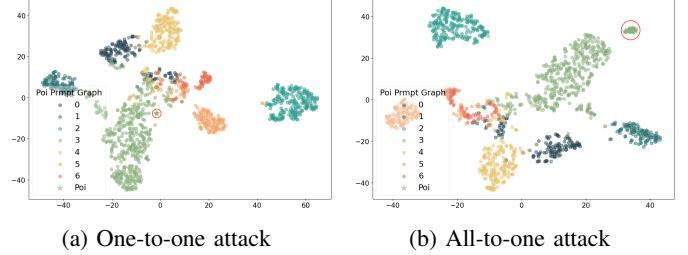


Fig. 23: Prompted node embedding with the “Interact” injection.

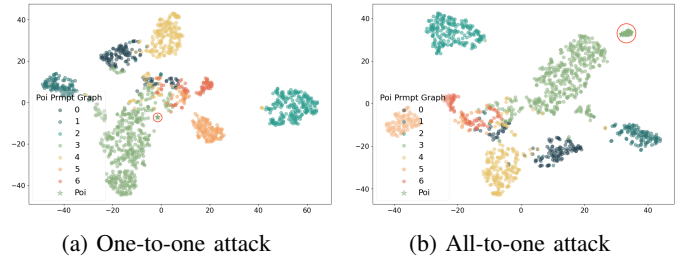


Fig. 24: Prompted node embedding with the “Modify” injection.